Cooperative control for self-organizing microgrids and game strategies for optimal dispatch of distributed renewable generations

Ali Maknouninejad, Wei Lin, Hendra G. Harno, Zhihua Qu & Marwan A. Simaan

Springer

Springer

ORIGINAL PAPER

Cooperative control for self-organizing microgrids and game strategies for optimal dispatch of distributed renewable generations

**Ali Maknouninejad · Wei Lin · Hendra G. Harno ·
Zhihua Qu · Marwan A. Simaan**

Abstract The small size, extensively dispersed and decentralized, and high penetration level of renewable energy sources in the future smart grids make the application of conventional optimal power flow (OPF) neither practical nor economical. In this paper, a practical approach is proposed to realize high penetration of distributed generators (DGs) by organizing them in some groups within a microgrid and dispatching the generated power aggregately. Each group may have virtual leaders which define the power policy of the group, and all other DGs cooperatively follow that policy. A fair utilization ratio is defined and will be introduced to the group by the virtual leaders. The utilization ratio indicates what percentage of the available power each DG has to feed to the grid, and this ratio will also be propagated within the group using cooperative control. As such, a smartgrid may treat microgrids as individually dispatchable loads or generators. Meanwhile, the interaction between each microgrid and the main grid can be formulated as a Stackelberg game. The main grid as the leader, by offering proper energy price to the micro grid, minimizes its cost and secures the power supply that the microgrid, as the follower, is willing to dispatch. It is shown that this game theoretic approach not only guarantees profit optimization, but also provides a convenient technique to optimize power flow from microgrids to

A. Maknouninejad · W. Lin · H.G. Harno · Z. Qu (✉) · M.A. Simaan
Department of EECS, University of Central Florida, Orlando, FL 32816, USA
e-mail: qu@eecs.ucf.edu

A. Maknouninejad
e-mail: alimaknouni@gmail.com

W. Lin
e-mail: w.lin2009@knights.ucf.edu

H.G. Harno
e-mail: h.g.harno@gmail.com

M.A. Simaan
e-mail: simaan@eecs.ucf.edu

the main grid. Numerical and simulation results for a case of study are provided to demonstrate the effectiveness of the proposed techniques.

Keywords Smartgrid · Microgrid · Distributed generator · Cooperative control · Game theory

1 Introduction

The global increase of electricity demand combined with both economical and environmental constraints of conventional energy sources such as fossil or nuclear energy, is putting more demand on finding alternative energy sources. Renewable energy sources are of special interest as alternative energy. This has lead to the outburst of the distributed generators (DGs) and smartgrid concepts. DGs have many different forms such as solar or wind energy, fuel cells or even small diesel generators. To increase the harness of alternative energy, DGs will be installed near the loads and be spread widely across the distribution network.

It is believed that the high penetration of DGs, will result in the reduction of power losses, voltage profile improvement, meeting future load demand, and optimizing the use of non-conventional energy sources [7]. However, more serious problems will arise if a decent control mechanism is not exploited. An improperly managed high PV penetration, may cause voltage profile disturbance, conflict with conventional network protection devices, interfere with transformer tap changers, and as a result, cause network instability.

Indeed, it is feasible to organize DGs in a microgrid structure which will be connected to the main grid through a point of common coupling (PCC). Microgrids are natural innovation zones for the smart grid because of their scalability and flexibility. A proper organization and control of the interaction between microgrid and smartgrid is a research challenge.

In this paper, a multilevel smartgrid control strategy is offered to provide solutions to both the DGs control in the microgrids and interaction management between the microgrids and the main grid as follows:

1. A microgrid needs to organize its DGs to realize predetermined objectives. The ultimate goal is to have DGs operate fairly together to help provide stability, to keep voltage profile within the acceptable range and to provide a desired power flow. DGs usually exploit the use of fast power electronic converters, inverters, for getting connected to the grid.

   Grid-tie inverters are at the heart of today's renewable energy conversion systems and future smart grids. These inverters convert the energy harnessed from the various renewable energy sources, such as wind, sun, etc., into a grid quality AC power that can be fed into the utility grid. As such, the appropriate control and management of inverters will have a significant effect on the performance of the microgrids.

   Currently, existing inverter control strategies include current source inverter (CSI) [3, 36], voltage/frequency droop control [12, 13], generator emulation control (GEC) [1], and cooperative control [34]. CSI mainly has the inverter feed all

its available power to the grid and has been shown to cause stability problems on high penetrations [5]. Different derivatives of droop control and GEC use communicationless control to imitate the behavior of synchronous generators. However, these controllers regulate their point of connection voltage and frequency without considering the effect or demands on other parts of the grid and this may cause some problems. For instance, they may cause conflict with the transformer tap changing voltage control mechanisms [5] or may disturb the voltage profile across long feeders.

As such, an appropriate control scheme extends far beyond just regulating inverters coupling point voltage and frequency. Cooperative control provides the possibility for different agents in a networked area operate together to realize some desired objectives [24] and already has been successfully applied to autonomous vehicle control [28]. The application of cooperative control for DGs operation on power systems was proposed in [34]. But it did not include main grid/microgrid interaction, neither considered the dynamics of the inverters. In this paper, cooperative control design based on inverter dynamics is proposed and is shown that based on the active power demand from the main grid, microgrid utilizes intermittent, asynchronous, and low bandwidth communication links and organizes DGs to work cooperatively together to fulfill the demand. Similarly, the excessive power capacity of DGs will be used to produce reactive power to regulate a critical point voltage which may be a farthest point on the microgrid or a bus with sensitive loads.

2. A proper interaction between the microgrid and the main grid is an important aspect of the smartgrid. A microgrid should look as a dispatchable load to the main grid and it is desired to have a power flow to the main grid to minimize the cost and also shave the peak of the load demand. In [34], assuming a certain power flow to the main grid is demanded, a PI controller was applied to regulate the power produced by DGs accordingly. However, this technique may be applied once the desired power flow is known. As such, another high level controller should be devised to properly search and come up with the most suitable power flow from the microgrid to the main grid, considering the different constraints including:

(i) Both the microgrid and the main grid should be able to optimize their profit or cost.

(ii) Improvement in the main grid generated power is an objective. It is desired to have less power fluctuations, which incur high stress and cost to the generators. To this end, the main grid generated power profile should be as smooth as possible. This means that the microgrids should assist the main grid to shave its power peak. To this end, microgrid may charge its storages when there is less power demand and release energy during peak hours.

The above requirements can be met by modeling the main grid-microgrid interaction as a game [6]. Game theory is briefly introduced in Sect. A.1. In terms of the conventional electric market, some of the previous works utilize different game theoretic approaches to deal with the optimal bidding strategy for the generating company, optimal load pricing, and reserve management problem. Towards this end, [8, 10, 11, 19, 25] focus on the Nash game, and [4, 16, 17, 35] focus on

the Stackelberg game. In terms of future smartgrid, [18] provided a demand-side management based on consumption scheduling game to optimize the energy cost and balance the load, and [33] analyzed the smartgrid management with multiple intelligent players. However, the interaction between the main grid and microgrid is an important aspect of the smartgrid, which has not been fully considered using a game theoretic approach.

In this paper, main grid-microgrid interaction is modeled as a Stackelberg game. Specifically, by offering proper energy price to the microgrid, the main grid as the leader, can minimize its cost function and secure the power supply that microgrids, as the follower, are willing to dispatch. Once receiving the offered price from the main grid, microgrids decide what percentage of the available power to dispatch and how much to store. It is shown that this technique not only is helpful in terms of optimizing the cost functions, but also helps a proper power flow from the microgrid to the main grid to reduce load stresses and shave the peak.

The rest of this paper is organized as follows. The proposed control strategy to be incorporated will be introduced and formulated in Sect. 2. The cooperative control of DGs, considering the dynamics of the inverters, will be discussed in Sect. 3. The required medium level control to manage microgrid aggregated power dispatch is introduced in Sect. 4. The Stackelberg game between the main grid and microgrids is formulated and solved in Sect. 5. Examples with related numerical and simulation results are presented for the purpose of illustration in Sect. 6.

2 Problem formulation

Figure 1 shows the typical block diagram of a smartgrid. A smartgrid consists of several generation sources including large scale renewable sources such as wind farms or solar farms, and conventional power stations. Small sized distributed generators, such as rooftop solar panels and home installed small wind turbines are also important elements of the smartgrid which will be able to provide a high aggregated power dispatch.

The best way to organize and control such highly dispersed and individually small sized generation is to group them in the form of microgrids [23], as shown in Fig. 1. Then, a cooperative low-level control is applied to organize and properly dispatch the DGs.

A smartgrid consists of several buses to which loads, conventional generators and microgrids may be connected. An example of a smartgrid based on IEEE 5-bus system is shown in Fig. 2, where a microgrid is connected to the bus 5. The dynamics of the synchronous generators are described as follows:

$$\begin{cases} \dot{\theta}_i = \omega_i \\ M_i \dot{\omega}_i = P_{Di} - P_{Gi} \end{cases} \quad i = 1, 2, \ldots N_b^t$$

On the buses to which microgrids are connected, the aggregated generation on the bus is considered in the above equation. The detailed model of an individual DG,
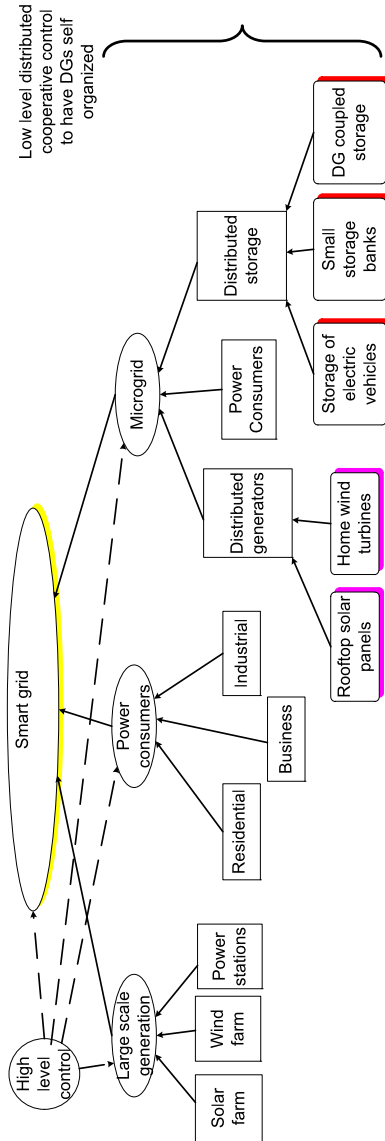
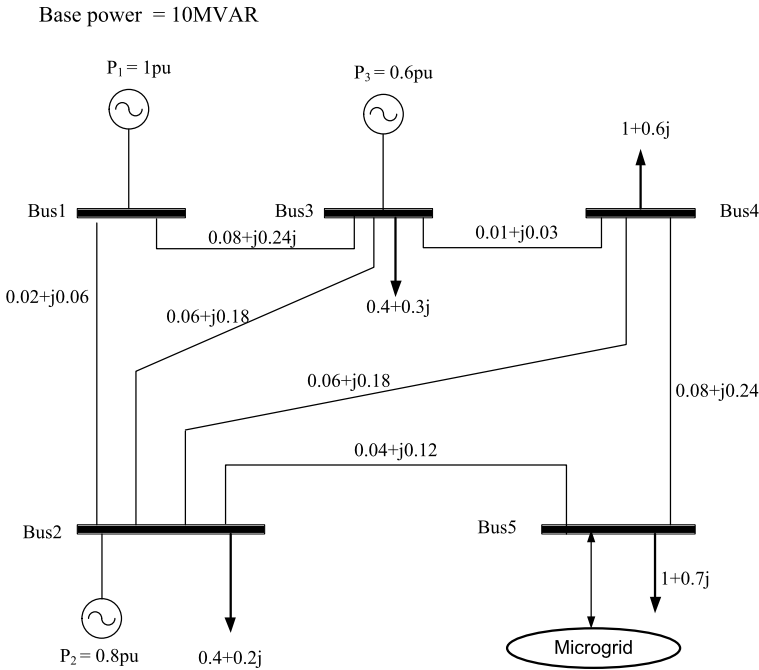**Fig. 1** Typical smartgrid block diagram

Fig. 2 A smartgrid diagram based on IEEE 5-bus system

operating inside the microgrid, is provided on Sect. 2.1. The power flows on the system buses are constrained by the following power flow equations:

$$\begin{cases} P_{Gi} - P_{Di} = \sum_{j \in N_b^t} V_i V_j [G_{ij} \cos \delta_{ij} + B_{ij} \sin \delta_{ij}] \\ Q_{Gi} - Q_{Di} = \sum_{j \in N_b^t} V_i V_j [G_{ij} \sin \delta_{ij} - B_{ij} \cos \delta_{ij}] \end{cases} \quad i, j = 1, 2, \ldots N_b^t \quad (1)$$

To encourage the DGs to produce renewable energy, the smartgrid provides incentives to the energy delivered by them. Thus, every DG tries to maximize its interest by more generation. However, in the utility market of a smartgrid, the desire of each participant to maximize its own profit needs to be coordinated or constrained to ensure the system operation and to minimize the overall cost.

The smartgrid control should be multilevel. On the microgrid level, DGs should be organized and cooperatively operate to satisfy desired power demands and maximize their profit. On the main grid level, main grid offers a power price to the microgrids to secure a desired power flow and meanwhile minimize its costs. Therefore, a high level control is needed to manage the interaction between the main grid and microgrids. The proposed control scheme problem is formulated in detail in Sects. 2.1–2.4.

2.1 Microgrid level distributed control

The small size of DGs and their potential high penetration in the future smartgrids, make the application of conventional optimal power flow (OPF) neither practical nor
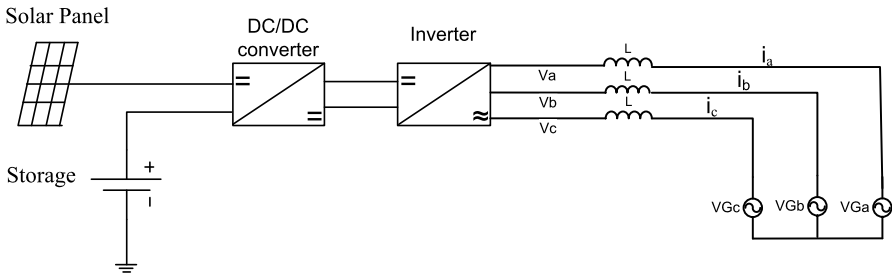
Fig. 3 Typical structure of a PV based DG, coupled to the grid using a three phase inverter

economical. When it comes to the control and management of such highly dispersed and small scale generators, organizing them in the form of microgrids is the viable solution. Microgrids are the innovation zone for a smartgrid as they provide flexibility and scalability to control DGs and realize smartgrid objectives.

In order to improve the performance of microgrids, such as flexibility and reliability, energy storages (batteries, super capacitors, etc.) will be available and bundled with DGs. As such, the available active power on the microgrid consists of both stored and renewable energy.

DGs are usually connected to the grid through fast responding DC/AC converters (inverters) [13]. The typical structure of a DG, coupled to the grid by an inverter, is shown in Fig. 3. Using PI controllers in the $d - q$ reference frame, the following state space equations are derived to describe the dynamics of the ith inverter:

$$\begin{cases} \dot{x}_i = A_i x_i + B_i u_i \\ y_i = C_i x_i, \end{cases} \tag{2}$$

where

$$x_i = \begin{bmatrix} \int (u_i - I_i) dt \\ I_i \end{bmatrix}, \qquad I_i = \begin{bmatrix} i_{di} \\ i_{qi} \end{bmatrix}, \qquad y_i = \begin{bmatrix} \alpha_{pi} \\ \alpha_{qi} \end{bmatrix}, \qquad u_i = \begin{bmatrix} u_{i1} \\ u_{i2} \end{bmatrix},$$

$$A_i = \begin{bmatrix} 0 & 0 & -1 & 0 \\ 0 & 0 & 0 & -1 \\ \frac{K_i}{L} & 0 & -\frac{K_p}{L} & 0 \\ 0 & \frac{K_i}{L} & 0 & -\frac{K_p}{L} \end{bmatrix}, \qquad B_i = \begin{bmatrix} 1 & 0 \\ 0 & 1 \\ \frac{K_p}{L} & 0 \\ 0 & \frac{K_p}{L} \end{bmatrix},$$

$$C_i = \begin{bmatrix} 0 & 0 & \frac{V_{Gi}}{P_i} & 0 \\ 0 & 0 & 0 & -\frac{V_{Gi}}{Q_i} \end{bmatrix}.$$

Here, I_i is the output current. It is noteworthy that all the measurements on the inverter are with respect to the voltage measured at the output terminal. As such, $V_{di} = V_{Gi}$ and $V_{qi} = 0$. Therefore, the output power of the ith inverter can be expressed as:

$$P_i = i_{di} V_{Gi}, \qquad Q_i = -i_{qi} V_{Gi}.$$

Typical three phase inverter dynamics and detailed space state model is derived in the Sect. A.2.

The maximum available active power of the ith unit is as follows:

$$\overline{P}_i = P_{DG_i} + P_{s_i}, \tag{3}$$

where $P_{DG_i}(k)$ is the available renewable power and P_{s_i} is the power from storage. Assuming E_{si} to be the existing stored energy of the ith unit, the maximum power provided by discharging this energy in time interval T is

$$P_{s_i} = E_{si}/T.$$

The microgrid power management should be in such a way not only meet certain power policies, but also provide the possibility that all DGs contribute equally. Therefore, fair utilization ratios, α_p and α_q, are introduced to determine how many percentage of the available active or reactive power is to be generated by every DG:

$$\alpha_{p_i} = \frac{P_i}{P_{DG_i} + P_{s_i}}. \tag{4}$$

Accordingly, the energy stored in the unit i at the end of time interval T is:

$$E_{si}(k + 1) = [1 - \alpha_{p_i}][P_{DG_i}(k)T + E_{si}(k)] \tag{5}$$

Assuming that the renewable power, P_{DG_i}, is constant during time interval T.

Equations (4, 5) indicate that when there is active power available, some part of it may be sent to the grid and the rest be stored.

Each inverter has a nominal power rating, S_i. If the active power generated by DG is less than this nominal rating, the excessive power capacity may be exploited to generate reactive power:

$$\begin{cases} \overline{Q}_i = \sqrt{S_i^2 - P_i^2} \\ Q_i = \alpha_{q_i} \overline{Q}_i, \end{cases} \tag{6}$$

where Q_i and $\overline{Q}_i$ are the generated and the maximum available reactive power of the ith unit respectively. Equation (6) indicates what percentage of the available reactive power is to be fed to the grid.

DGs should utilize communication links to communicate and converge to the same operating point, α_p^{ref} and α_q^{ref}, provided by the virtual leaders. Virtual leaders may be some of the inverters that have access to the higher level control and can calculate the required utilization ratios. However, communication links may be asynchronous, intermittent, of time-varying topology, and of low bandwidth. The instantaneous communication topology is defined by the following matrix:

$$S(t) = \begin{bmatrix} s_{00}(t) & s_{01}(t) & s_{02}(t) & \cdots & s_{0n}(t) \\ s_{10}(t) & s_{11}(t) & s_{12}(t) & \cdots & s_{1n}(t) \\ s_{20}(t) & s_{21}(t) & s_{22}(t) & \cdots & s_{2n}(t) \\ \vdots & \vdots & \vdots & \ddots & \vdots \\ s_{n0}(t) & s_{n1}(t) & s_{n2}(t) & \cdots & s_{nn}(t) \end{bmatrix} \tag{7}$$

In (7), $s_{ii} = 1$ for all i; $s_{ij} = 1$ if the output of the jth DG is known to the ith DG at time t, and $s_{ij} = 0$ if otherwise. In (7), unit 0 is assumed to be the virtual leader.

Virtual leader needs to have access to either the top level control agent, power flow information or voltage profile of the lines. As such, if any of the operating modules have access to such information, it may acquire the position of the virtual leader and as such, (7) is reduced to:

$$S(t) = \begin{bmatrix} s_{11}(t) & s_{12}(t) & \cdots & s_{1n}(t) \\ s_{21}(t) & s_{22}(t) & \cdots & s_{2n}(t) \\ \vdots & \vdots & \ddots & \vdots \\ s_{n1}(t) & s_{n2}(t) & \cdots & s_{nn}(t) \end{bmatrix} \tag{8}$$

The communication matrix should be piecewise constant over time, and the corresponding sequence should be sequentially complete [34]. The communication topology and frequency rates affect the system convergence rate. Therefore, they should be considered when designing the control laws.

As such, the first problem is for a group of DGs, G, how to design control inputs u_i in (2) such that they all converge to the proper α_p^{ref} and α_q^{ref}:

$$\begin{cases} \alpha_{p_i} \to \alpha_p^{ref} \\ \alpha_{q_i} \to \alpha_q^{ref} \end{cases} \quad \forall i \in G$$

2.2 Medium level control and optimization

The solution to the first problem provides the possibility for the DGs on the microgrid to converge to a desired α_p^{ref} and α_q^{ref}. However, there should be a control mechanism to search for the right utilization ratios and satisfy power objectives. In this paper and as proposed in [34], maintaining the downstream active power at a desired value and regulating the voltage of a critical point are the power objectives. Such critical points may be nodes farthest from the point of common coupling (PCC) or where more critical and sensitive loads are located.

Following (3), for a group of DGs, G, in any microgrid of interest, the maximum available active power to be dispatched at hour k is:

$$\sum_{j \in G} [P_{DG_j}(k) + E_{sj}(k-1)/T].$$

The relation between the aggregated active power generated, P_{DG}^a, at hour k and the available renewable power, P_{DG_j}, and the storage energy, E_{sj}, of the jth unit are described as follows:

$$P_{DG}^a(k) = \begin{cases} \alpha_p(k) \sum_{j \in G} [P_{DG_j}(k) + E_{sj}(k-1)/T] \\ \quad \text{if active power is available,} \\ \in (-\infty, 0] \quad \text{otherwise.} \end{cases} \tag{9}$$

Accordingly, the aggregated energy stored in the microgrid, at the end of the kth hour is:

$$E(k) = \begin{cases} [1 - \alpha_p(k)] \sum_{j \in G} [P_{DG_j}(k)T + E_{sj}(k-1)] \\ \quad \text{if active power is available} \\ \sum_{j \in G} [E_{sj}(k-1)] - T P_{DG}^a \quad \text{otherwise} \end{cases} \tag{10}$$

Equations (9, 10) indicate that when there is active power available, some part of it may be sent to the grid and the rest be stored. Otherwise, some power may be absorbed from the grid to charge the storages.

Following (6):

$$Q_{DG}^a(k) = \alpha_q^{ref}(k) \sum_{j \in G} \overline{Q}_j(k). \tag{11}$$

Therefore, there should be a mechanism to provide a α_q^{ref} in (11) to control reactive power generation properly to regulate the critical point voltage.

The active power flow of the microgrid at bus i to the main grid is expressed as follows:

$$P_{\mu_i}(k) = P_{DG_i}^a(k) - P_{L_i}^\mu(k) - P_{losses_i}^\mu(k). \tag{12}$$

For simplicity, microgrid losses, $P_{losses_i}^\mu$, and load, $P_{L_i}^\mu$, may be lumped together.

To secure a desired power dispatch from the microgrid, $P_{\mu_i}^{ref}$, main grid proposes an energy price, β_i. This price is subject to the generation and load demand and is expected to increase during peak hours and be less at night and when there is less demand in general. As such, the microgrid cost function for the hours k up to N is calculated as follows:

$$J_{\mu_i}(\beta_i(k), P_{\mu_i}(k)) = \sum_{l=k}^{N} \beta_i(l) P_{\mu_i}^{ref}(l), \tag{13}$$

where J_{μ_i} is the cost function which shows the microgrid profit by generating power. At every hour, k, based on the available power, load and the predicted generation and load for the upcoming hours, the microgrid tries to search for the best $P_{\mu_i}^{ref}$ to maximize its profit. Then, the required DG active power generation, $P_{DG_i}^a$, is calculated using (12). Substituting this $P_{DG_i}^a$ into (9), provides the $\alpha_{p_i}^{ref}$. However, in case the PV generation or load fluctuate, or real values deviated from the predicted ones, the $\alpha_{p_i}^{ref}$ needs to be updated to keep the same power flow, $P_{\mu_i}^{ref}$.

As such, the second problem is how each microgrid finds the best possible $P_{\mu_i}^{ref}$ at every hour k to maximize cost function (13), update $\alpha_{p_i}^{ref}$ to secure this power flow and how to search for the proper $\alpha_{q_i}^{ref}$ to regulate the critical point voltage to the $V_c^{ref} = 1$ P.U.

2.3 Main grid optimization

In general, at the main grid level with N_b^t buses, the real-time OPF problem of dispatching P_{μ_i} is to minimize the following cost-to-go function for total power system at hour k:

$$J_t(k) = \sum_{i=1}^{N_b^t} \sum_{l=k}^{N} \left[a_i P_{G_i}(l) + \beta_i(l) P_{\mu_i}^{ref}(l) \right], \tag{14}$$

where N indicates the final stage (in this case time = 24 P.M) and a is the per unit power price of the conventional generations, P_{G_i}, on the main grid.

The above optimization is subject to the power flow constraints of (1), which are non-linear and solved numerically [14]. As in the energy market only the active power flow is of interest, DC power flow which is a simplification of (1) can be used. The DC power flow neglects active power losses, assumes voltage angle differences are small and that the magnitude of nodal voltages are equal. As a result, the only variables are voltage angles and active power injections. Therefore, the problem becomes linear and there is no need for iterations. These assumptions cause errors as compared to the original power flow equations (1). Subject to keeping the error below 5%, the following constraints should be met [26]:

1. Voltage angle differences, δ_{ij}, be less than 5°,
2. Lines impedances X/R ratio be greater than 2,
3. For a X/R ratio of 2, the voltage standard deviation be less than 0.012.

In case the above constraints are satisfied, the DC power flow may be used instead of (1) as follows:

$$P^a_{G_i}(k) - P^a_{D_i}(k) = \sum_{j=1}^{N^t_b} B_{ij}\delta_{ij}(k) \quad i = 1, \ldots, N^t_b \tag{15}$$

The optimization of (14), is also subject to the steady state constraints:

$$\begin{aligned}\underline{P}_{G_i}(k) \le P_{G_i}(k) \le \overline{P}_{G_i}(k), \\ \underline{P}_{\mu_i}(k) \le P_{\mu_i}(k) \le \overline{P}_{\mu_i}(k)\end{aligned} \tag{16}$$

and thermal constraints:

$$-\underline{T}_i \le T_i(k) \le \overline{T}_i. \tag{17}$$

Note that $P^a_{G_i}$ in (15) may be equal to 0 if there is no generation, equal to P_{G_i} if there is only conventional generation, equal to P_{μ_i} if there is only microgrid connected to the bus, or equal to $P_{G_i} + P_{\mu_i}$ if there are both conventional and microgrid generation.

As such, the third problem is subject to constraints of (15, 16, 17), how the main grid should propose the power price, β_i, to the microgrids to minimize its cost function (14) and secure a proper power dispatch, P_{μ_i}, from the microgrids.

2.4 Interaction between main grid and microgrid

Within a smartgrid, there is an interaction between the main grid and the microgrids. The main grid tries to motivate microgrids to generate power by offering appropriate energy price, β_i, to them, and at the same time, tries to minimize its cost function (14). On the other hand, microgrids try to maximize their profits of (13) by dispatching appropriate active power P_{μ_i}. Since the optimization objectives of the main grid and the microgrids are contradictory, such a problem can be formulated as a noncooperative game [2]. The concept of noncooperative game is addressed in more detail in Sect. A.1. For our problem, because the main grid announces hourly energy price first and the microgrids dispatch active power after that, the game is indeed a Stackelberg game with the main grid as the leader and the microgrids as the followers. Hence, a
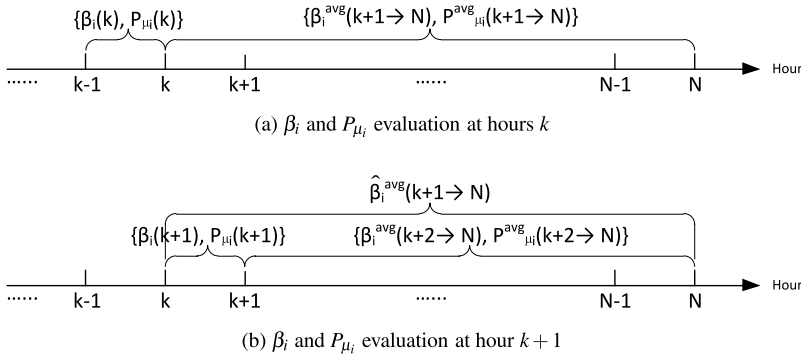
(a) β_i and P_{μ_i} evaluation at hours k

(b) β_i and P_{μ_i} evaluation at hour $k+1$

Fig. 4 A simplified game model

Stackelberg solution can be obtained to secure demanded power from the main grid and improve the performance indices (13) and (14).

By predicting possible power price β_i and power dispatch P_{μ_i} from hour 1 up to N, it is possible to play this game for N hours at once. However, there will be a large number of possible solutions to evaluate. For example, if $N = 24$, and there are five possible P_{μ_i} at every hour k, then there will be 5^{24} combinations of P_{μ_i} (and the corresponding β_i) to perform the whole game. This approach is thus impractical.

Also, at every hour k, the calculation of performance indices (13) and (14) requires information for all the hours k up to N. However, only data of the current hour, k, are known and for the remaining hours of $(k + 1)$ up to N, the predicted PV generation and load are available. Yet, the prospective values of $\beta_i(k + 1 \rightarrow N)$ and $P_{\mu_i}(k + 1 \rightarrow N)$ neither are known nor have predicted profiles. These issues will then be difficult to handle if the game problem is to be solved effectively. Hence, a simplified game from hour k to N is proposed to carry out the original optimization with respect to the performance indices (13) and (14).

A modification on (13) and (14) is then necessary in order to suit the simplified game approach, which is illustrated in Fig. 4. In this case, the predicted PV generation, load profiles and the current hour choices of $\beta_i(k)$ and $P_{\mu_i}(k)$ are utilized; and the average values of the parameters for the upcoming hours are calculated and used to estimate the performance indices from hour $(k + 1)$ to N. Thus, the performance indices (13) and (14) are modified as

$$
\begin{aligned}
J_\mu(\beta_i(k), P_{\mu_i}(k)) \\
= \beta_i(k) P_{\mu_i}(k) + (N - k)\beta_i^{avg}(k + 1 \rightarrow N) P_{\mu_i}^{avg}(k + 1 \rightarrow N),
\end{aligned} \tag{18}
$$

and

$$
\begin{aligned}
J_t(\beta_i(k), P_{\mu_i}(k)) = a_i P_{G_i}(k) + \beta_i(k) P_{\mu_i}(k) \\
+ (N - k)\big[a_i^{avg}(k + 1 \rightarrow N) P_{G_i}^{avg}(k + 1 \rightarrow N) \\
+ \beta_i^{avg}(k + 1 \rightarrow N) P_{\mu_i}^{avg}(k + 1 \rightarrow N)\big].
\end{aligned} \tag{19}
$$

The optimizations of (18) and (19) are subject to the condition that the storage level of the microgrid, should return to its initial value after N hours. This require-

ment leads to a constraint on the average increment or decrement stored energy, ΔE_i^{avg}, as follows:

$$\Delta E_i^{avg}(k \rightarrow N) = \frac{\Delta E_i(k) + [N - (k)]\Delta E_i^{avg}(k + 1 \rightarrow N)}{N - (k + 1)},$$
$$\forall k \in [1, N - 2], \tag{20}$$

where

$$\Delta E_i(k + 1) = E_i(k + 1) - E_i(k). \tag{21}$$

Equation (20) is a recursive expression. $\Delta E_i^{avg}(k \rightarrow N)$ is calculated on the previous hour, $k - 1$. It represents the hourly change of average stored energy from hour k to N. The consistency of this average for hour k and $k + 1$ is imposed by (20). Then, for any proposed choice of $\Delta E_i(k)$ by the microgrids, a $\Delta E_i^{avg}(k + 1 \rightarrow N)$ is derived for the next hour.

When the game is not played, there is no storage involved and hence, the aggregated output power $P_{DG_i}^a(k)$ is equal to the sum of the available power:

$$P_{DG_i}^a(k) = \sum_{j=1}^{N_{DG_i}} P_{DG_{ij}}(k), \tag{22}$$

where $P_{DG_{ij}}$ is the available renewable power of the jth DG in a microgrid connected to the ith bus. However, when the game is played between the main grid and the microgrids, the aggregated output power $P_{DG_i}^a(k)$ is represented as follows:

$$P_{DG_i}^a(k) = \sum_{j=1}^{N_{DG_i}} P_{DG_{ij}}(k) - \frac{\Delta E_i(k)}{T}, \tag{23}$$

where the second term on the right hand side of (23) is accounted for the energy storage change within time period T. Thus, by substituting (23) into (12), the constraint (20) can then be rewritten in terms of P_{μ_i} and $P_{\mu_i}^{avg}$ as follows:

$$P_{\mu_i}^{avg}(k + 1 \rightarrow N) = \frac{P_{\mu_i}(k + 1) + [N - (k + 1)]P_{\mu_i}^{avg}(k + 2 \rightarrow N)}{N - k},$$
$$\forall k \in [1, N - 1]. \tag{24}$$

Although the consistency of $\beta_i^{avg}(k \rightarrow N)$ and $\beta_i^{avg}(k + 1 \rightarrow N)$ is not imposed, but it can be verified according to

$$\begin{cases} \hat{\beta}_i^{avg}(k + 1 \rightarrow N) = \frac{\beta_i(k+1) + [N-(k+1)]\beta_i^{avg}(k+2 \rightarrow N)}{N-k}, & \forall k \in [1, N-1] \\ \beta_i^{avg}(k + 1 \rightarrow N) = \hat{\beta}_i^{avg}(k + 1 \rightarrow N). \end{cases} \tag{25}$$

The term $\hat{\beta}_i^{avg}(k + 1 \rightarrow N)$ in (25) refers to the re-evaluation of $\beta_i^{avg}(k + 1 \rightarrow N)$ at hour $(k + 1)$, using $\beta_i(k + 1)$ and $\beta_i^{avg}(k + 2 \rightarrow N)$, which are obtained from the game at hour $(k + 1)$ as shown in Fig. 4b. Evaluating (25) analytically is not straightforward and it can be checked numerically for any case of interest.

As such, the forth problem is how to calculate the performance indices (18) and (19) and play the game.

3 Cooperative control

Utilizing the available communication links, DGs are to converge to the utilization ratios α_p^{ref} and α_q^{ref}, provided by the virtual leaders. However, the communication links may have limited bandwidth, be intermittent and asynchronous. So a proper control scheme needs to be applied which can tolerate the changes in a distribution network which may have time varying topologies, its local communication can be intermittent and of minimum bandwidth. Cooperative control has the advantage that utilizing such non consistent communication links, can have a group of agents/modules exhibit cooperative behaviors and make the system act as one group. Cooperative control has been already applied to autonomous vehicle control [28] and its basic application for DG control on power systems was introduced in [34]. In this section, to facilitate all DGs to self-organize, the design of cooperative control with respect to the dynamics of inverters is provided. The cooperative control law for the system of (2) for a group of N_{DG} inverters is as follows.

$$\begin{cases} u_{i1} = \frac{L}{K_p V_{Gi}} \{ \bar{P}(d_{i0}\alpha_p^{ref} - \alpha_{pi} + \sum_{j=1}^{N_{DG}} d_{ij}\alpha_{pj}) \\ \qquad - [(\dot{V}_{Gi} - V_{Gi}\frac{K_P}{L})x_{3i} + V_{Gi}\frac{K_i}{L}x_{1i}]\} \\ u_{i2} = \frac{L}{K_p V_{Gi}} \{ -\bar{Q}(d_{i0}'\alpha_q^{ref} - \alpha_{qi} + \sum_{j=1}^{N_{DG}} d_{ij}'\alpha_{qj}) \\ \qquad - [(\dot{V}_{Gi} - V_{Gi}\frac{K_P}{L})x_{4i} + V_{Gi}\frac{K_i}{L}x_{2i}]\}, \end{cases} \tag{26}$$

where

$$d_{ij} = \frac{s_{ij}}{\sum_{j=0}^{N_{DG}} s_{ij}}, \quad i = 0, 2, \dots N_{DG} \tag{27}$$

s_{ij} is a generic entry of matrix S defined in (7); d_{i0} and d_{i0}' are defined similar to (27) and for them, s_{i0}, s_{i0}' are 1 if DG_i has communication with the active and reactive virtual leaders, respectively. Otherwise, $s_{i0}, s_{i0}' = 0$. Equation (26) provides the solution to the problem in Sect. 2.1.

4 Medium level control

At every hour k, the $P_{\mu_i}^{ref}$ is determined by a higher level control which will be covered in Sect. 5. Then, based on (9) and (12), $\alpha_{p_i}^{ref}$ is calculated which will be propagated across the microgrids through cooperative control, discussed in Sect. 2.1. In case microgrid load changes, or the generated renewable energy fluctuates due to environmental conditions, the $P_{DG_i}^a$ and as a result, P_{μ_i} will vary according to (12). As such, a medium level controller should be used to secure the designated power flow, P_{μ_i}, regardless of such disturbances.

As discussed in [34], an integrator controller may be used to update the $\alpha_{p_i}^{ref}$ accordingly as follows and shown on Fig. 5a.

$$\dot{\alpha}_{p_i}^{ref} = k_p(P_{\mu_i}^{ref} - P_{\mu_i}). \tag{28}$$

(a) Active power regulation mechanism (b) Reactive power regulation mechanism
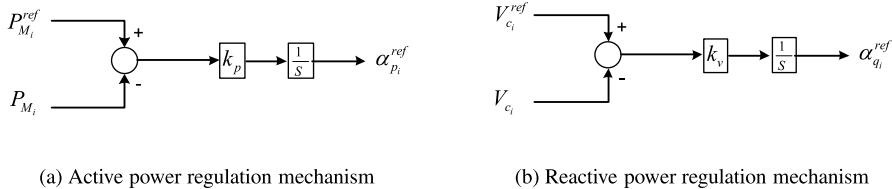
Fig. 5 Active/reactive power regulation mechanism

In case the load/PV severely fluctuates, a new game should be played by the top level controller to propose relevant P_{μ_i} and α_{p_i}.

To regulate the critical point voltage, a similar mechanism may be used as follows and shown in Fig. 5b:

$$\dot{\alpha}_{q_i}^{ref} = k_v (V_c^{ref} - V_{c_i}), \tag{29}$$

where $V_c^{ref} = 1$ P.U.

The closed loop system for any microgrid of interest, can be expressed by substituting (26) in (2) as follows:

$$\dot{z}_i = k_c \left[-z_i + d_{i0}z_0 + \sum_{j=1}^{N_{DG}} d_{ij}z_j \right],$$

where $z_i = \alpha_{pi}$, the fair utilization ratio of the ith inverter. As such, the overall dynamics of the microgrid system can be expressed as follows:

$$\dot{z}_0 = k_p \left[P_\mu^{ref} - P_\mu(z_1, \dots, z_{N_{DG}}, X_p) \right], \tag{30}$$

$$\dot{z}_i = k_c \left[-z_i + d_{i0}z_0 + \sum_{j=1}^{N_{DG}} d_{ij}z_j \right], \tag{31}$$

$$0 = g_p(P_1, \dots, P_{N_{DG}}, X_P), \tag{32}$$

where $z_0 = \alpha_p^{ref}$ and (30) is a restatement of (28) for a desired microgrid. Equation (32) is the power flow equation of the system. The stability of the closed loop system is proved based on the following lemma.

Lemma 1 *If $A \in \mathbb{R}^{N_{DG} \times N_{DG}}$ is a row-stochastic, connected matrix and can be expressed as*

$$A = D + D_0,$$

where $D \in \mathbb{R}^{N_{DG} \times N_{DG}}$ and $D_0 = diag\{d_{01}, d_{02}, \dots, d_{0N_{DG}}\}$ are non-negative, then

 (i) *matrix $(D - I)$ is Hurwitz,*
(ii) *matrix $(I - D)^{-1}$ exists and is non-negative.*

The proof of the above lemma is given in Sect. A.3.

Theorem 1 *For a microgrid system whose dynamics is given by* (30)–(32), *if the following conditions are satisfied*

(1) k_p/k_c *is sufficiently small,*
(2) *Communication among the DGs are cumulatively connected (sequential complete),*
(3) $|\sin(\delta_i - \delta_j)| \ll |\cos(\delta_i - \delta_j)|,$

the system is asymptotically stable in the sense that $z_i \to z_0$.

The proof of this theorem is also given in Sect. A.3. Equations (28), (29) and Theorem 1 provide the solution to the problem stated in Sect. 2.2.

Furthermore, for system

$$\dot{z}_i = k_c \left(w_i + d_{i0}z_0 + \sum_{j=1}^{N_{DG}} d_{ij}z_j \right) \quad i = 1, 2, \ldots, N_{DG}; \tag{33}$$

the following theorem shows that

$$w_i = w_i^* = -z_i \quad i = 1, 2, \ldots, N_{DG}; \tag{34}$$

form a Nash equilibrium with respect to certain performance indices.

Theorem 2 *If the system dynamics is given by* (33), *then* $w_i = w_i^*$ *in* (34) *for* $i = 1, 2, \ldots, N_{DG}$ *form a Nash equilibrium with respect to the following performance indices*

$$J_i = \frac{1}{2} \sum_{j=1}^{N_{DG}} z_j^2(t_f) + \int_{t_0}^{t_f} \left[q_i(z_0, z_1, \ldots, z_{N_{DG}}) + \frac{k_c}{2} w_i^2 \right] dt \tag{35}$$

for $i = 1, 2, \ldots, n$, *where*

$$q_i = \frac{k_c}{2} z_i^2 - \sum_{j=1}^{N_{DG}} k_c z_j^2 + \sum_{j=1}^{N_{DG}} k_c d_{j0} z_j z_0 + \sum_{j=1}^{N_{DG}} \left[k_c z_j \left(\sum_{k=1}^{N_{DG}} d_{jk} z_k \right) \right] \tag{36}$$

for $i = 1, 2, \ldots, n$.

For the detailed proof, please refer to Sect. A.4.

Remark 1 According to the nature of Nash equilibrium, by suitably choosing k_c, performance index (35) can be assigned to each DG so that they have no choice but to stick to the Nash equilibrium.

5 Game solution for smartgrid

To solve the game problem presented in Sect. 2.4, the following steps are carried out to calculate performance indices J_μ in (18) and J_t in (19).

1. The active power $P_{\mu_i}(k)$, flowing from the microgrid (on the ith bus) to the main grid at hour k is given by (12).
2. Assume that the storage level of a microgrid should return to its initial value after N hours, then the average active power from hour $(k+1)$ to N, $P_{\mu_i}^{avg}(k+1 \to N)$, is given by:

$$P_{\mu_i}^{avg}(k+1 \to N) = \text{avg}[P_{\mu_i}(k+1 \to N)] + \frac{\sum_{l=1}^{k} \Delta E_i(l)}{N-k}, \qquad (37)$$

where $\text{avg}[P_{\mu_i}(k+1 \to N)]$ is the predicted average power flow from historical data without considering the storage.
3. Conventional generation $P_{G_i}(k)$ (on the ith bus) at hour k is given by

$$P_{G_i}(k) = P_{D_i}(k) - P_{\mu_i}(k). \qquad (38)$$

And the predicted average generation from hour $(k+1)$ to N is given by

$$P_{G_i}^{avg}(k+1 \to N) = P_{D_i}^{avg}(k+1 \to N) - P_{\mu_i}^{avg}(k+1 \to N), \qquad (39)$$

where $P_{D_i}^{avg}(k+1 \to N)$ is the predicted average demand from hour $(k+1)$ to N.
4. Using $P_{G_i}(k)$ given by (38), $\beta_i(k)$ is computed by the following equation:

$$\beta_i(k) = \beta_0 \left[1 + \eta_i(k) \frac{P_{G_i}(k) - P_{G_i}^*(k)}{P_{G_i}^*(k)} \right], \qquad (40)$$

where $P_{G_i}^*$ is the optimal operation power of the conventional generator (on the ith bus), β_0 is a known base price (when $P_{G_i} = P_{G_i}^*$, $\beta_i = \beta_0$), and $\eta_i(k)$ is a variable, which the main grid perturbs to find different energy price offers to play the game. Basically, equation (40) means that if P_{G_i} is larger than $P_{G_i}^*$, the main grid should increase the price β_i to motivate the DGs to produce more energy, and if the P_{G_i} is less than $P_{G_i}^*$, the price β_i should be decreased to encourage DGs to store more energy. This helps the generators operate near the optimal operation power, $P_{G_i}^*$.
5. Similarly, $P_{G_i}^{avg}(k+1 \to N)$ in (39) will be used to calculate $\beta_i^{avg}(k+1 \to N)$ as follows:

$$\beta_i^{avg}(k+1 \to N) = \beta_0 \left[1 + \eta_i(k) \frac{P_{G_i}^{avg}(k+1 \to N) - P_{G_i}^*(k)}{P_{G_i}^*(k)} \right].$$

Through the above steps, for every possible choice of $\Delta E_i(k)$ and $\eta_i(k)$, the corresponding values of $P_{\mu_i}(k)$, $P_{\mu_i}^{avg}(k+1 \to N)$, $\beta_i(k)$, and $\beta_i^{avg}(k+1 \to N)$ are obtained, and hence cost functions (18) and (19) can be calculated.

In order to find the game solution, a matrix game can be constructed. Specifically, suppose that there exist M_1 choices of $\eta_i(k)$,

$$\{\eta_i(k, 1), \eta_i(k, 2), \ldots, \eta_i(k, M_1)\},$$

and M_2 choices of $\Delta E_i(k)$, which result in M_2 choices of $P_{\mu_i}(k)$,

$$\{P_{\mu_i}(k, 1), P_{\mu_i}(k, 2), \ldots, P_{\mu_i}(k, M_2)\}.$$

Hence, a matrix game can be constructed as Table 1, where values of $\eta_i(k)$ are located at the far left column and values of $P_{\mu_i}(k)$ are located at the far top row. The other entries are pairs of $\{J_t, J_{\mu_i}\}$ based on corresponding $\eta_i(k)$ and $P_{\mu_i}(k)$.

Table 1 Matrix game between the main grid and a microgrid

$\eta_i(k)$	$P_{\mu_i}(k)$		
	$P_{\mu_i}(k, 1)$	$\cdots$	$P_{\mu_i}(k, M_2)$
$\eta_i(k, 1)$	$\begin{cases} J_t[\eta_i(k, 1), P_{\mu_i}(k, 1)], \\ J_{\mu_i}[\eta_i(k, 1), P_{\mu_i}(k, 1)] \end{cases}$	$\cdots$	$\begin{cases} J_t[\eta_i(k, 1), P_{\mu_i}(k, M_2)], \\ J_{\mu_i}[\eta_i(k, 1), P_{\mu_i}(k, M_2)] \end{cases}$
$\vdots$	$\vdots$	$\ddots$	$\vdots$
$\eta_i(k, M_1)$	$\begin{cases} J_t[\eta_i(k, M_1), P_{\mu_i}(k, 1)], \\ J_{\mu_i}[\eta_i(k, M_1), P_{\mu_i}(k, 1)] \end{cases}$	$\cdots$	$\begin{cases} J_t[\eta_i(k, M_1), P_{\mu_i}(k, M_2)], \\ J_{\mu_i}[\eta_i(k, M_1), P_{\mu_i}(k, M_2)] \end{cases}$

Table 2 Matrix game for Example 1, where $\{\star, \star\}$ stands for $\{J_\mu, J_t\}$

$\eta_i(k)$	$P_{\mu_i}(k)$	
	0.8	1
1	{8, 10}	{10, 9}
1.2	{7, 5}	{6, 7}

Using such a table, either the Nash equilibrium or the Stackelberg solution can be found. Since the main grid acts as a leader and the microgrids act as the followers, the search algorithm for Stackelberg solution is presented here (please refer to Sect. A.5 for the counterpart of Nash equilibrium).

1. For each $\eta_i(k, j)$ for $j = 1, 2, \ldots, M_1$, a corresponding $P_{\mu_i}(k)$ can be found such that $J_{\mu_i}[\eta_i(k, j), P_{\mu_i}(k)]$ is maximized and that $P_{\mu_i}(k)$ is denoted as $P_{\mu_i}^S[\eta_i(k, j)]$.
2. The Stackelberg solution of the main grid is $\eta_i(k, l)$ for some l such that

$$J_t[\eta_i(k, l), P_{\mu_i}^S(\eta_i(k, l))] \leq J_t[\eta_i(k, j), P_{\mu_i}^S(\eta_i(k, j))]$$

for all $j = 1, 2, \ldots, M_1$.

To illustrate this algorithm, a simple example is provided as follows:

Example 1 Suppose that the matrix game is shown in Table 2.

The Stackelberg solution with the main grid as the leader is obtained as follows:

1. For $\eta_i(k) = 1$, $P_{\mu_i}(k) = 1$ maximizes J_{μ_i} because

$$J_{\mu_i}(1, 1) = 10 \text{ is greater than } J_{\mu_i}(1, 0.8) = 8.$$

For $\eta_i(k) = 1.2$, $P_{\mu_i}(k) = 0.8$ maximizes J_{μ_i} because

$$J_{\mu_i}(1.2, 0.8) = 7 \text{ is greater than } J_\mu(1.2, 1) = 6.$$

2. Since

$$J_t(1.2, 0.8) = 5 \text{ is less than } J_t(1, 1) = 9,$$

the Stackelberg solution of the main grid is $\eta_i(k) = 1.2$.

The Nash equilibrium counterpart of this particular example is also shown in Sect. A.5. Note that for a game problem, a Nash equilibrium may happen to be the same as the Stackelberg solution, which is the case in Sect. 6.

This section provided solution to problems stated on Sects. 2.3 and 2.4.

6 Illustrative examples

To illustrate the smartgrid control algorithm discussed earlier, the design and application of game and cooperative control for the case of a microgrid versus one bus main grid is discussed in this section as shown in Fig. 6. A modified version of the bus system proposed by IEEE 399-1997 standard is used to represent the microgrid. There are 5 feeders and 8 DGs are distributed across the microgrid with a total of 8MVA generation capacity. The microgrid connects to the main grid through point of common coupling (PCC).

Main grid is represented by a single bus into which an aggregated load and conventional generator is connected. Two set of examples are provided in this section. At Sect. 6.1, simulations for evaluating the performance of the cooperative control are provided. Section 6.2 shows the game approach and numerical results for managing the smartgrid.

6.1 Application of cooperative control on microgrid

In this example, eight DGs are spread across the microgrid and are organized by the cooperative control. DG8 is the agent which runs game negotiations with the main grid and hence, is the active power virtual leader. Reactive power policy is to regulate the critical point voltage, which is L21 in this case. As such, DG3 which is connected to L21 and measures its voltage, is the virtual reactive power leader. Simulations are performed using Simulink Simpower System Toolbox.

To show the effect of communication frequency, Fig. 7a shows the DG4 α_p convergence to $\alpha_p^{ref} = 0.6$ under different frequency rates. Figure 7b also shows the voltage of critical point voltage. As expected, higher frequency rates result in faster convergence rate. The other major factor affecting the performance of the system, is communication topology (8) through which inverters communicate. Three different communication topologies have been investigated here. In all cases

$$S(t) = 0, \quad t \in ((k-1)T_c + 0^+, kTc], \quad T_c = \frac{1}{f_c},$$

and for $[(k-1)T_c, (k-1)T + 0^+)$:

$$
\begin{cases}
S_0(t), & \text{Global connectivity; when all inverters have access to others information;} \\
S_1, & \text{A randomly selected topology;} \\
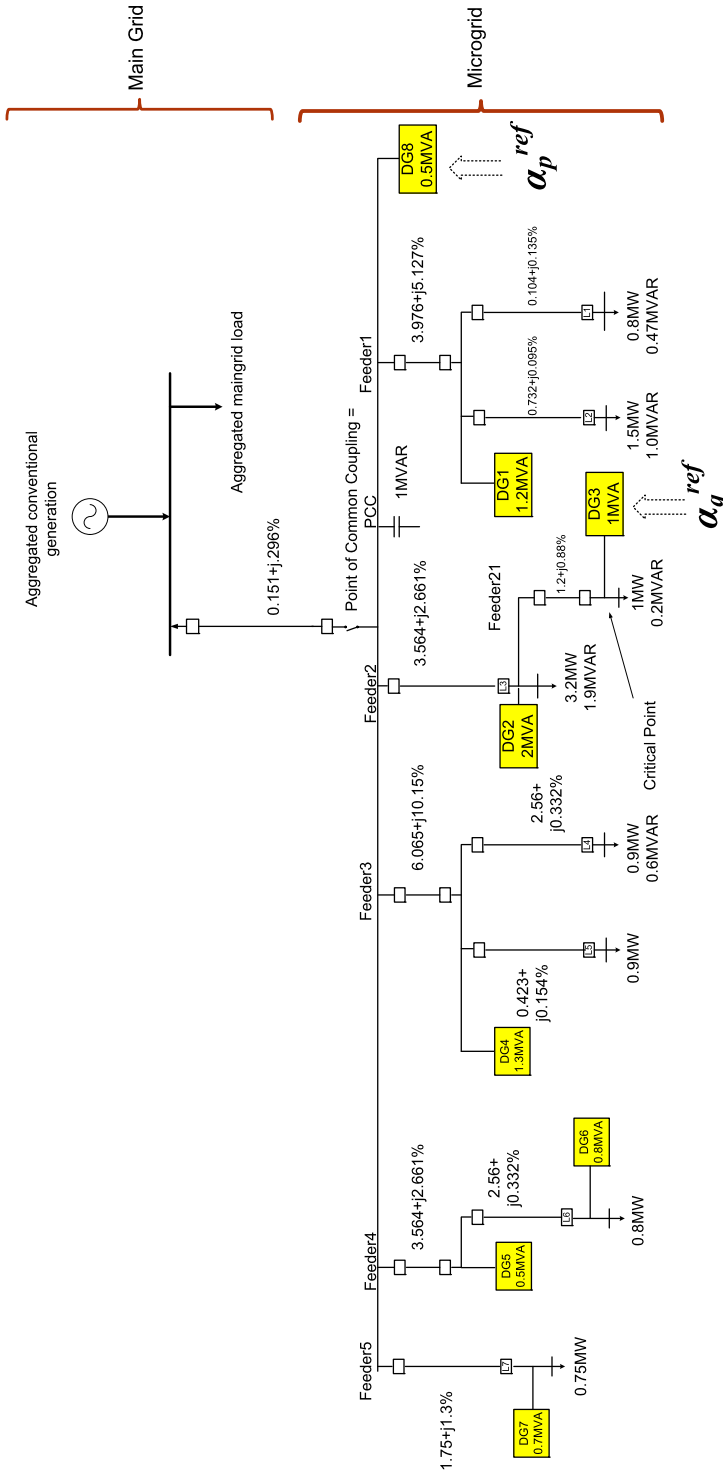S_2, & \text{Neighboring connectivity; when only access to neighbors is possible.}
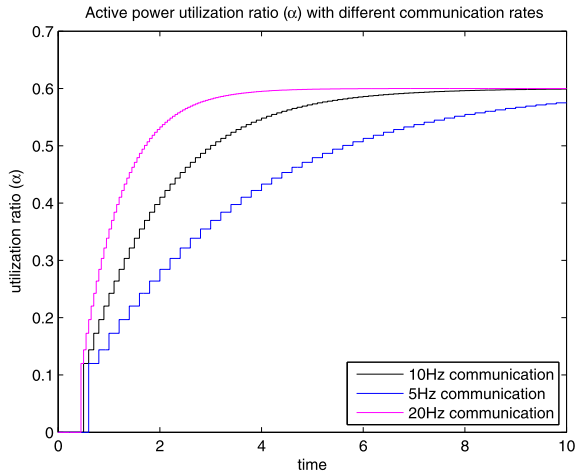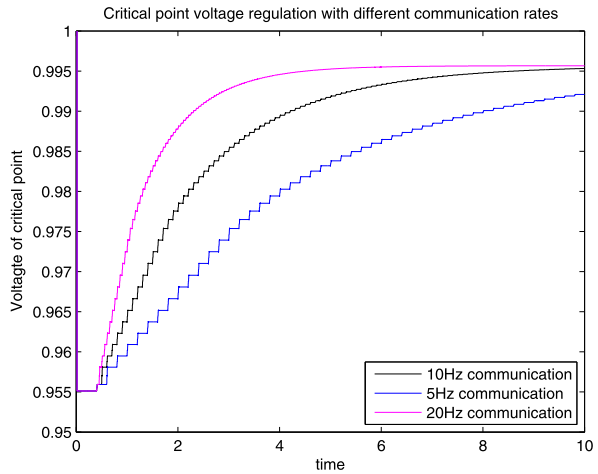\end{cases}
$$

Fig. 6 Case of study smartgrid

Fig. 7 Cooperative control performance under different frequency rates

Active power utilization ratio (α) with different communication rates

(a) DG4 utilization ratio (α_p) convergence rate

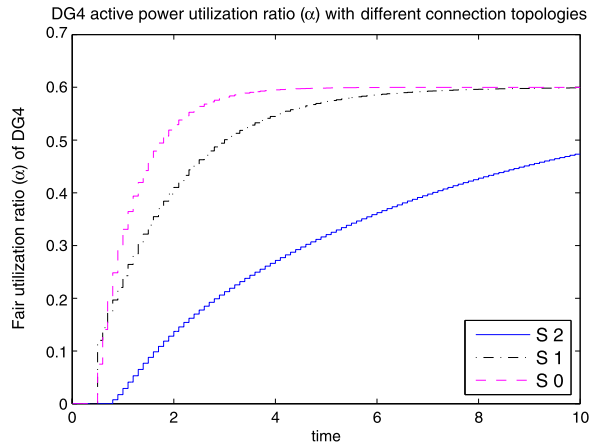Critical point voltage regulation with different communication rates
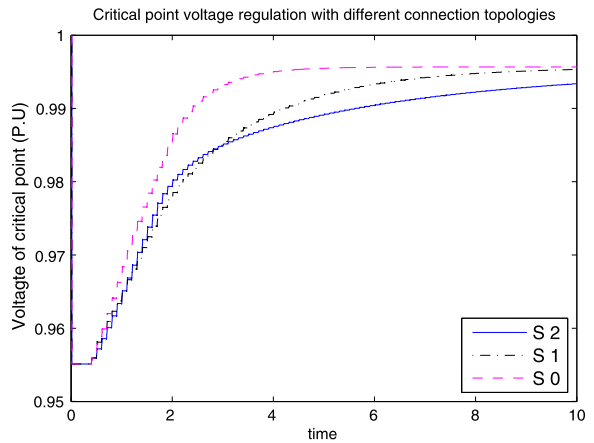
(b) Voltage of critical point

where:

$$S_0(t) = [1], \qquad S_1(t) = \begin{bmatrix} 1 & 0 & 0 & 1 & 0 & 1 & 0 & 0 \\ 0 & 1 & 0 & 0 & 0 & 0 & 1 & 1 \\ 0 & 0 & 1 & 0 & 1 & 0 & 1 & 0 \\ 1 & 0 & 0 & 1 & 1 & 1 & 0 & 1 \\ 0 & 0 & 1 & 1 & 1 & 0 & 0 & 0 \\ 1 & 0 & 0 & 1 & 0 & 1 & 0 & 0 \\ 0 & 1 & 1 & 0 & 0 & 0 & 1 & 0 \\ 0 & 1 & 0 & 1 & 0 & 0 & 0 & 1 \end{bmatrix},$$

Fig. 8 Cooperative control effect with different communication topologies

DG4 active power utilization ratio (α) with different connection topologies

(a) DG4 utilization ratio (α_p) convergence rate

Critical point voltage regulation with different connection topologies

(b) Voltage of critical point

$$S_2(t) = \begin{bmatrix} 1 & 1 & 0 & 0 & 0 & 0 & 0 & 0 \\ 1 & 1 & 1 & 0 & 0 & 0 & 0 & 0 \\ 0 & 1 & 1 & 1 & 0 & 0 & 0 & 0 \\ 0 & 0 & 1 & 1 & 1 & 0 & 0 & 0 \\ 0 & 0 & 0 & 1 & 1 & 1 & 0 & 0 \\ 0 & 0 & 0 & 0 & 1 & 1 & 1 & 0 \\ 0 & 0 & 0 & 0 & 0 & 1 & 1 & 1 \\ 0 & 0 & 0 & 0 & 0 & 0 & 1 & 1 \end{bmatrix}.$$

Figure 8a and 8b show the simulation results with the aforementioned communication topologies. It is seen that with more communication links, faster responses are achieved. It is also noticed that if communication is limited to only neighboring units, convergence rate is decreased. Having connection with some modules rather far away, also improves the convergence rate.
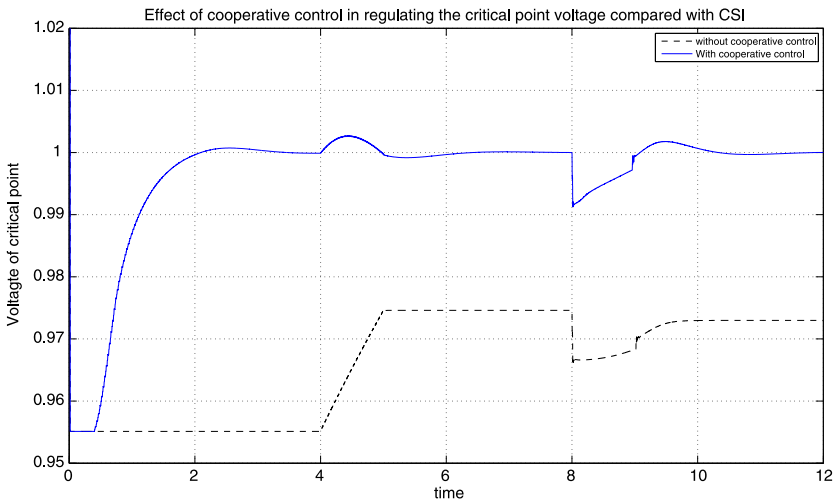
Fig. 9 Cooperative control and CSI comparison in regulating the critical point voltage

Figure 9 shows a side by side comparison between cooperative control and conventional current source inverters (CSI). CSI is the conventional grid-tie inverter controller which feeds all the available active power of the inverters to the grid. For the cooperative control, $\alpha_p^{ref} = 0.6$ is chosen and α_q^{ref} is adaptively controlled to maintain the line voltage. This figure illustrates the superiority of cooperative control versus CSI in regulating line voltage and damping the voltage dips.

Up to $t = 4$ s, there is no active power available. So CSI inverters become idle while the cooperative control helps voltage regulation by adaptively controlling the DG VAR generation. From $t = 4$ s up to $t = 5$ s, available active power rises linearly from 0 up to 1 P.U. This causes voltage increase. Voltage rise by CSI is not controlled and is not enough to regulate the line voltage. On the other hand, cooperative control takes care of the voltage boost and regulates the voltage back by adjusting the reactive power generation accordingly. At $t = 8$ s, a 300 kVA asynchronous machine starts on feeder 1 and causes the voltage dip. Cooperative control is shown to be effective in damping this voltage dip and rather quickly takes the voltage back.

6.2 Interaction between main grid and microgrid: Stackelberg game approach

The game approach proposed in Sect. 5 will be illustrated here by applying it for the main grid-microgrid case of Fig. 6. Predicted PV generation and loads are provided in the Sect. A.6. At each hour, based on the real time and predicted generation/load, the cost functions (13) & (14) are calculated for the different prices and power flows offered by the main grid and microgrid, respectively. Then, the Stackelberg solution with the main grid as the leader is found.

It is assumed that the microgrid has 1 P.U storage capacity. Hence, it can supply its local loads for about one hour in case of main grid disconnection. The initial storage is 0.5 P.U. Charge and discharge rates are limited to 0.25 P.U. Storage level at the end of the day (hour 24) should return to its initial value. The storage here makes

Table 3 Cost function optimizations

	$J_\mu (1-24)$	$J_t (1-24)$
Without game	6.4682	84.0155
With game	10.5716	81.6979

Table 4 The values of power flow P_μ^{ref} and α_p^{ref}

Hour	P_μ^{ref}	α_p^{ref}	Hour	P_μ^{ref}	α_p^{ref}
1	−0.4142	−0.5000	13	0.3123	0.4074
2	−0.3822	−0.3333	14	0.3519	0.4402
3	−0.1162	0	15	0.4113	0.5463
4	−0.0602	0	16	−0.0163	0.2352
5	0.0064	0.0481	17	0.0038	0.2446
6	−0.0746	0.0647	18	−0.0483	0.2500
7	0.1910	0.2853	19	−0.0670	0.3333
8	0.2360	0.3656	20	−0.0691	0.5000
9	0.3138	0.4239	21	−0.0490	1.0000
10	0.2494	0.3674	22	−0.2596	–
11	0.3485	0.4074	23	−0.4606	–
12	0.3998	0.4221	24	−0.4142	−1.0000

the difference when the game is played or not. If there is no game in the smartgrid control, all the available active power is fed to the grid. When the game is played, to optimize the cost functions, sometimes some power is used to charge the storages (this power will come either from renewable sources (DGs) or the main grid) and sometimes storages are discharged. It is expected that during the night time when there is less power demand, microgrid buys power from the main grid to charge and during the day time when there is power peak demand, storages are released. As such, power peak shaving and improved power flow is expected.

As explained earlier in Sect. 5, the game is played between η in (40) and microgrid power flow P_μ. Table 3 shows the improvements in the cost functions by running the game for 24 hours. It is seen that the game has reduced the main grid cost J_t and increased the microgrid profit J_μ. The power flow of the main grid is shown in Fig. 10a. The dashed line is the power flow without game and the solid one is the one with game. It is seen that the game has increased the load when originally was less load and has decreased the load when originally power demand is high. It is clear that this game strategy not only has helped cost optimization, but also resulted in peak power shave and improved power flow. For this particular case, the Nash solution was also considered which showed the same results of the Stackelberg solution.

Playing a 24-hours game, results in P_μ^{ref} and α_p^{ref} as presented in Table 4. Note that at hour-22 and hour-23, the values of α_p^{ref} (computed using (9) and (10)) do not exist because the active power is not available during those hours. Based on the data in Table 4, Fig. 10b is then presented to graphically show a 24-hour profile of the power flow P_μ^{ref}. Positive value of P_μ^{ref} means that power flows from the

Fig. 10 The effect of the
proposed game approach on
power flow and peak power
shaving
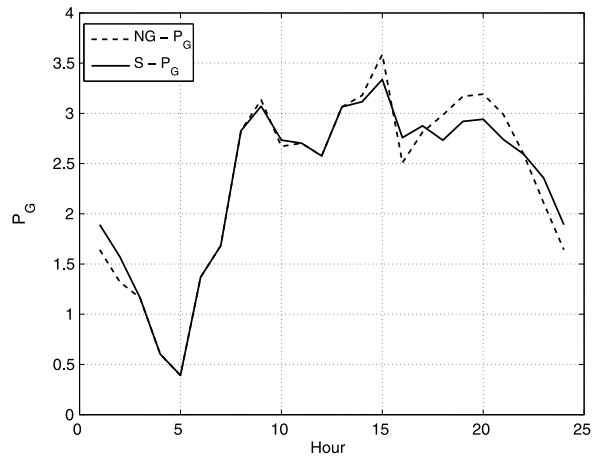
(a) Main grid power flow
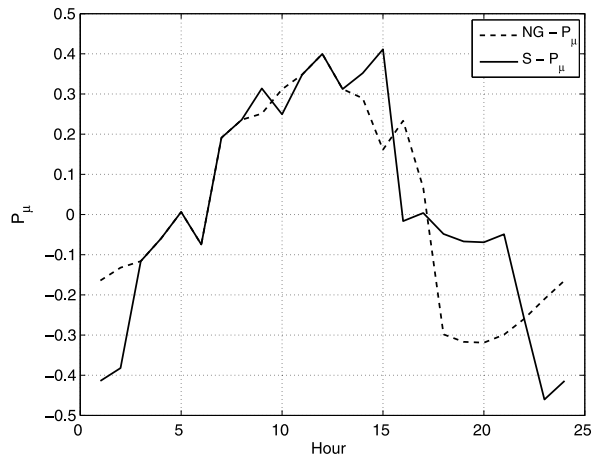
(b) Microgrid power flow

microgrid to the main grid. It is shown that at night hours and when there is less
power demand, power flow to the main grid has decreased as compared with the time
that there is no game. That is because, at these time periods, when less power prices
are offered by the main grid, the game results in charging the storages so that they
may be released at the peak hours when power prices increase. As an illustration, the
game procedure for hour-1 is shown in the Sect. A.7 and the process is similar for the
next hours.

Equation (25) is used to verify the accuracy of the estimations provided in
Sect. 2.4. The values of β, β^{avg} and $\hat{\beta}^{avg}$ are presented in Table 5; where β^{avg} and
$\hat{\beta}^{avg}$ match well except at hour-11, 20 and 22 where there are discrepancies. The
mismatch is less than 15% and as such, the estimation of (18, 19) has an acceptable
accuracy.

Table 5 The energy prices: β_i, β_i^{avg}, and $\hat{\beta}_i^{avg}$

Hour	β_i	β_i^{avg}	$\hat{\beta}_i^{avg}$	Hour	β_i	β_i^{avg}	$\hat{\beta}_i^{avg}$
1	7.2204	7.9977	7.9977	13	11.6484	10.0497	10.0497
2	6.6757	8.0578	8.0578	14	11.9087	9.8638	9.8638
3	5.9779	8.1569	8.1569	15	13.0408	9.5108	9.5108
4	5.0247	8.3135	8.3135	16	10.0867	9.4388	9.4388
5	4.6663	8.5054	8.5054	17	10.6869	9.2605	9.2605
6	6.3299	8.6263	8.6263	18	9.9557	9.1447	9.1447
7	6.8643	8.7299	8.7299	19	10.9106	8.7915	8.7915
8	8.8114	8.7248	8.7248	20	11.0179	8.2349	8.0783
9	9.2273	8.6913	8.6913	21	8.6638	7.8831	7.8831
10	8.6529	8.6941	8.6941	22	8.4187	7.6153	6.8357
11	8.6000	8.7013	10.1040	23	8.0102	5.6613	5.6613
12	9.1565	10.1829	10.1829	24	5.6613	–	–

7 Conclusions

In this paper, a multilevel control strategy for managing a smartgrid is proposed. On microgrid level, cooperative control is used to organize and have DGs operate and converge to the same reference utilization ratios. At the medium level control, there are virtual leaders for active and reactive powers, respectively. The active power virtual leader searches for the appropriate active power utilization ratio, α_p^{ref}, to secure a desired power flow, P_μ^{ref}, from microgrid towards the main grid. The reactive power virtual leader tries to adjust the reactive power utilization ratio, α_q^{ref}, to regulate the critical point voltage of the microgrid. Meanwhile, the top level control is the one handling the interaction between the main grid and the microgrids. The interests of the main grid and microgrids are different. The main grid tries to minimize its cost while has to secure a demanded power flow from the microgrids. It does that by proposing proper energy prices to the microgrids. Microgrids try to maximize their profits by properly handling their renewable power generation and storage. This is formulated as a Stackelberg game problem, in which the main grid as the leader, announces its hourly energy prices and the microgrids as the followers, have to decide the amount of power to dispatch. It is shown that this game strategy not only optimizes the performance indices of both sides, but also improves power flow on the main grid and microgrid in term of peak power shaving.

Appendix

A.1 Introduction to the game theory

The game models strategic situations, in which an individual's success in making choices depends on the choices of others [20]. The modern game theory was first proposed by von Neuman and Morganstern in 1944. Basically, there are two major types of game. One is the cooperative game, where players collaborate with each other to achieve a common goal. The other is the non-cooperative game, which was developed by Nash in 1950s [21, 22], where each individual pursues its own interest or objective. For non-cooperative game, most of the results are summarized in [2]. In the non-cooperative game, if the players make their decisions simultaneously, then the game is called Nash game, and if the players make their decisions sequentially, then the game is called Stackelberg. The Stackelberg game was first established by the German economist, Heinrich von Stackelberg [32], and was extended to dynamic case by Simaan and Cruz [30, 31].

In a n-player Nash game, the strategy set $\{\gamma_1^N, \gamma_2^N, \ldots, \gamma_n^N\}$ for the n players is called a *Nash equilibrium* if and only if the following inequalities hold.

$$J_1(\gamma_1^N, \gamma_2^N, \ldots, \gamma_n^N) \le J_1(\gamma_1, \gamma_2^N, \ldots, \gamma_n^N),$$

$$J_2(\gamma_1^N, \gamma_2^N, \ldots, \gamma_n^N) \le J_2(\gamma_1^N, \gamma_2, \ldots, \gamma_n^N),$$

$$\vdots$$

$$J_n(\gamma_1^N, \gamma_2^N, \ldots, \gamma_n^N) \le J_n(\gamma_1^N, \gamma_2^N, \ldots, \gamma_n)$$

where $\gamma_1, \gamma_2, \ldots, \gamma_n$ are the decision variables for the n players belonging to the strategy space $\Gamma_1 \times \Gamma_2 \times \cdots \times \Gamma_n$ of all the admissible strategies, and $J_i(\gamma_1, \gamma_2, \ldots, \gamma_j, \ldots, \gamma_n)$ is the objective function or performance index for the ith player. The philosophy of the Nash equilibrium is that if the players' strategies form a Nash equilibrium, then no player intends to unilaterally change its strategy. If it does so, its objective function or performance index will worsen.

In a 2-player Stackelberg game, the strategy set $\{\gamma_1^S, \gamma_2^S\}$ is a *Stackelberg solution* with player 1 as the leader if and only if

$$\gamma_1^S = \arg\min_{\gamma_1 \in \Gamma_1} J_1(\gamma_1, \gamma_2(\gamma_1)) \quad \text{and} \quad \gamma_2^S = \gamma_2(\gamma_1^S),$$

where

$$\gamma_2(\gamma_1) = \arg\min_{\gamma_2 \in \Gamma_2} J_2(\gamma_1, \gamma_2).$$

The philosophy of the Stackelberg solution is that if the leader knows the optimal response of the follower, then it can play the Stackelberg strategy to optimize its objective function or performance index.

A.2 Inverter model

The system equation of Fig. 3 is as follow:

$$\begin{cases} V_{abc} = L\frac{di_{abc}}{dt} + V_{Gabc} \\ V_{abc} = K V_{c_{abc}}, \end{cases} \tag{41}$$

where K is the inverter gain and $V_{c_{abc}}$ is the overall controller output which is applied to the inverter. In power systems, it is customary to take variables in the $d - q$ reference frame and have calculation in terms of the $d - q$ variables. That is because sinusoidal variables turn into constants at the $d - q$ frame and this makes it easy to work, especially makes the application of simple PI controllers viable [3, 12, 36]. Applying the park transformation on the above equations provides the $d - q$ equivalent equations [12, 29]:

$$\frac{di}{dt} = \begin{bmatrix} 0 & \omega \\ -\omega & 0 \end{bmatrix} i + \frac{1}{L}(KV_c - V_G), \tag{42}$$

where

$$i = [i_d \quad i_q]^T, \qquad V_c = [V_{cd} \quad V_{cq}]^T, \qquad V_G = [V_{Gd} \quad V_{Gq}]^T.$$

Here, i is the output current, V_c is the input voltage command to the inverter, K is the inverter PWM gain, and V_G is the grid voltage at the inverter terminals.

The model (42) indicates that current components $i_{d,q}$ are coupled through ωi_d and ωi_q terms. This coupling can be eliminated by introducing the new variables V, as given by:

$$V = KV_c - V_G + \omega L[i_q \quad -i_q]^T, \tag{43}$$

where $V = [V_d \quad V_q]^T$. Substituting (43) in (42) yields:

$$\frac{di}{dt} = \frac{1}{L}V$$

This equation represents decoupled $i_{d,q}$ currents. Once the decoupled variables have been defined as in (43), a PI controller may be applied to control the overall system. This system block diagram is shown in Fig. 11.

Combining the inverter plant, decoupling section and controller in Fig. 11, inverter state space dynamic model of (2) is obtained.
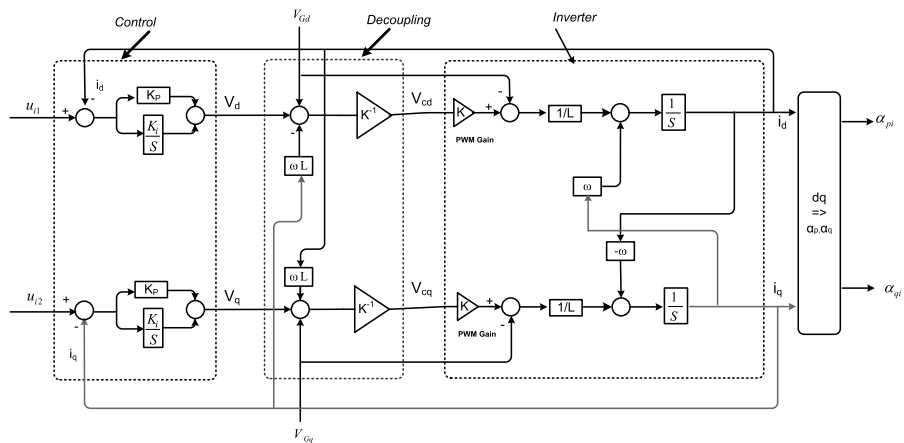

Fig. 11 Inverter model block diagram with PI control

A.3 Proofs of Lemma 1 and Theorem 1

The proof of Lemma 1 is given as follows.

Proof For (i), a square matrix is called a Hurwitz matrix if all its eigenvalues have strictly negative real parts [15]. Toward that, since A is row-stochastic and connected, the spectral radius $\rho(A)$ is equal to 1. Suppose that the eigenvalues of A are $\lambda_1, \ldots, \lambda_{N_{DG}}$. Then, the eigenvalues of $(I - A)$ are

$$1 - \lambda_1, \ldots, 1 - \lambda_{N_{DG}}.$$

Hence, the eigenvalues of $(I - A)$ are either zero or have positive real parts, and matrix $(I - A)$ is called a singular M-matrix [27]. According to Corollary 4.33 in [27], matrix

$$I - A + D_0$$

is a non-singular M-matrix. Since

$$I - A + D_0 = I - D - D_0 + D_0 = I - D,$$

matrix $(I - D)$ is a M-matrix. Therefore, $(D - I)$ is Hurwitz.

For (ii), since $(I - A)$ is a singular M-matrix, according to Theorem 4.27(c) in [27],

$$(I - A + D_0)^{-1} = (I - D)^{-1}$$

exists and is non-negative for positive diagonal matrix D_0. $\qquad\square$

The proof of Theorem 1 is presented as follows:

Proof The equilibrium of the system (30) and (31) is obtained by setting the right hand side of them to zero, that is, in vector form,

$$0 = P_\mu^{ref} - P_\mu(z_1, \ldots, z_{N_{DG}}, X_p), \qquad (44)$$

$$0 = - \begin{bmatrix} z_1 \\ z_2 \\ \vdots \\ z_{N_{DG}} \end{bmatrix} + \begin{bmatrix} d_{10} \\ d_{20} \\ \vdots \\ d_{N_{DG}0} \end{bmatrix} z_0 + \begin{bmatrix} d_{11} & \cdots & d_{1N_{DG}} \\ \vdots & \ddots & \vdots \\ d_{N_{DG}1} & \cdots & d_{N_{DG}N_{DG}} \end{bmatrix} \begin{bmatrix} z_1 \\ z_2 \\ \vdots \\ z_{N_{DG}} \end{bmatrix}. \qquad (45)$$

From (44), it is straight forward to obtain

$$P_\mu(z_1, \ldots, z_{N_{DG}}) = P_\mu^{ref},$$

which gives the equilibrium of z_0 denoted by z_0^*. From (45), if $d_0 = [d_{10} \ d_{20} \cdots d_{N_{DG}0}]^T$ and $D = [d_{ij}] \in \mathbb{R}^{N_{DG} \times N_{DG}}$ for $i, j = 1, 2, \ldots, N_{DG}$, then (45) can be expressed as

$$(-I + D) \begin{bmatrix} z_1 \\ z_2 \\ \vdots \\ z_{N_{DG}} \end{bmatrix} + d_0 z_0 = 0. \qquad (46)$$

Then, based on (27), one can verify the following relationship:

$$d_0 = (I - D)\mathbf{1}_{N_{DG}}, \tag{47}$$

where $\mathbf{1}_{N_{DG}}$ is a N_{DG}-by-1 vector with all the elements being equal to 1. Substituting (47) into (46) yields

$$(-I + D)\left(\begin{bmatrix} z_1 \\ z_2 \\ \vdots \\ z_{N_{DG}} \end{bmatrix} - \begin{bmatrix} z_0 \\ z_0 \\ \vdots \\ z_0 \end{bmatrix}\right) = 0 \quad \Longrightarrow \quad \begin{cases} z_1 = z_0 \\ z_2 = z_0 \\ \vdots \\ z_{N_{DG}} = z_0. \end{cases}$$

Therefore, the equilibrium of the system is given by

$$\begin{cases} z_0 = z_0^* \\ z_1 = z_0^* \\ \vdots \\ z_{N_{DG}} = z_0^*. \end{cases}$$

Near the equilibrium, linearizing the system (44) and (45) yields

$$\begin{cases} \dot{z}_0 = -k_p \sum_{j=1}^{N_{DG}} e_j(z_j - z_0^*) \\ \dot{z}_i = k_c[-z_i + d_{i0}z_0 + \sum_{j=1}^{N_{DG}} d_{ij}z_j], \end{cases} \tag{48}$$

where

$$e_j = \left.\frac{\partial P_\mu}{\partial z_j}\right|_{z_j = z_0^*} > 0, \quad \forall j = 1, 2, \dots, N_{DG}.$$

The derivatives at the equilibrium is positive because in the microgrid, P_μ increases as z_j increases. Applying the following coordinate transformations

$$\begin{cases} x_0 = z_0 - z_0^* \\ x_1 = \begin{bmatrix} z_1 - z_0^* \\ z_2 - z_0^* \\ \vdots \\ z_{N_{DG}} - z_0^* \end{bmatrix} \end{cases}$$

and denoting $\tau = k_c t$, the linearized system (48) can be expressed as

$$\begin{bmatrix} \frac{dx_0}{d\tau} \\ \frac{dx_1}{d\tau} \end{bmatrix} = \begin{bmatrix} 0 & -\frac{k_p}{k_c}e^T \\ d_0 & D - I \end{bmatrix} \begin{bmatrix} x_0 \\ x_1 \end{bmatrix}, \tag{49}$$

where $e = [e_1 \cdots e_{N_{DG}}]^T$. Since k_p/k_c is sufficiently small, the dynamics of x_1 is much faster than that of x_0. According to singular perturbation theory [9], if x_0 would be constant, then x_1 will be asymptotically stable and converge to

$$x_1 = -(D - I)^{-1} d_0 x_0, \tag{50}$$

since $(D - I)$ is Hurwitz from (i) in Lemma 1. Substituting (50) to the dynamics of x_0 in (49) yields

$$\frac{dx_0}{d\tau} = \frac{k_p}{k_c} e^T (D - I)^{-1} d_0 x_0. \tag{51}$$

According to (ii) in Lemma 1, $(D - I)^{-1}$ is a non-positive matrix. Since $\frac{k_p}{k_c}$, e^T, and d_0 are all positive, $\frac{k_p}{k_c} e^T (D - I)^{-1} d_0$ is negative. Hence, x_0 is asymptotically stable and converge to 0. Therefore, $z_i \to z_0$ for $i = 1, 2, \ldots, N_{DG}$. □

A.4 Proof of Nash equilibrium

Proof of Theorem 2 is presented as follows.

Proof Consider the following Lyapunov functions

$$V = \frac{1}{2} \sum_{j=1}^{N_{DG}} z_j^2.$$

Differentiating V yields

$$
\begin{aligned}
\dot{V} &= \sum_{j=1}^{N_{DG}} z_j \dot{z}_j \\
&= \sum_{j=1}^{N_{DG}} \left[k_c z_j \left(w_j - w_j^* - z_j + d_{j0} z_0 + \sum_{k=1}^{N_{DG}} d_{jk} z_k \right) \right] \\
&= \sum_{j=1, j \neq i}^{N_{DG}} [k_c z_j (w_j - w_j^*)] + k_c z_i (w_i - w_i^*) - \sum_{j=1}^{N_{DG}} k_c z_j^2 + \sum_{j=1}^{N_{DG}} k_c d_{j0} z_j z_0 \\
&\quad + \sum_{j=1}^{N_{DG}} \left[k_c z_j \left(\sum_{k=1}^{N_{DG}} d_{jk} z_k \right) \right] \\
&= \sum_{j=1, j \neq i}^{N_{DG}} [k_c z_j (w_j - w_j^*)] + k_c z_i (w_i - w_i^*) - \sum_{j=1}^{N_{DG}} k_c z_j^2 + \sum_{j=1}^{N_{DG}} k_c d_{j0} z_j z_0 \\
&\quad + \sum_{j=1}^{N_{DG}} \left[k_c z_j \left(\sum_{k=1}^{N_{DG}} d_{jk} z_k \right) \right] \\
&\quad + \frac{k_c}{2} (w_i - w_i^*)^2 - \frac{k_c}{2} (w_i - w_i^*)^2.
\end{aligned}
\tag{52}
$$

Since

$$
\begin{aligned}
\frac{k_c}{2} (w_i - w_i^*)^2 &= \frac{k_c}{2} w_i^2 + \frac{k_c}{2} (w_i^*)^2 - k_c w_i w_i^* \\
&= \frac{k_c}{2} w_i^2 + \frac{k_c}{2} z_i^2 + k_c w_i z_i,
\end{aligned}
\tag{53}
$$

substitute (53) into (52) yields

$$
\dot{V}_i = \sum_{j=1, j \neq i}^{N_{DG}} [k_c z_j (w_j - w_j^*)] + k_c z_i (w_i - w_i^*) - \sum_{j=1}^{N_{DG}} k_c z_j^2 + \sum_{j=1}^{N_{DG}} k_c d_{j0} z_j z_0
$$

$$+ \sum_{j=1}^{N_{DG}} \left[k_c z_j \left(\sum_{k=1}^{N_{DG}} d_{jk} z_k \right) \right]$$

$$+ \frac{k_c}{2}(w_i - w_i^*)^2 - \frac{k_c}{2} w_i^2 - \frac{k_c}{2} z_i^2 - k_c w_i z_i$$

$$= \sum_{j=1, j\neq i}^{N_{DG}} [k_c z_j (w_j - w_j^*)] + \frac{k_c}{2}(w_i - w_i^*)^2 - \frac{k_c}{2} w_i^2 - q_i(z_0, z_1, \ldots, z_{N_{DG}}),$$

where q_i is defined in (36). By integrating the above equation over $[t_0, t_f]$ and using (35), we have

$$J_i = V_i(t_0) + \int_{t_0}^{t_f} \left[\frac{k_c}{2}(w_i - w_i^*)^2 + \sum_{j=1, j\neq i}^{N_{DG}} k_c z_j (w_j - w_j^*) \right] dt. \qquad (54)$$

Since (54) is applicable for all $i = 1, 2, \ldots, N_{DG}$, we can conclude that

$$J_i(w_1^*, w_2^*, \ldots, w_i^*, \ldots, w_{N_{DG}}^*) \leq J_i(w_1^*, w_2^*, \ldots, w_i, \ldots, w_{N_{DG}}^*)$$

for all $i = 1, 2, \ldots, N_{DG}$. Therefore, $(w_1^*, w_2^*, \ldots, w_{N_{DG}}^*)$ form a Nash equilibrium. $\qquad \square$

A.5 Search algorithm for Nash equilibrium

Search algorithm for Nash equilibrium is as follows:

1. For each $\eta_i(k, j)$ for $j = 1, 2, \ldots, M_1$, $P_{\mu_i}(k, l)$ can be found for some l such that $J_{\mu_i}[\eta_i(k, j), P_{\mu_i}(k)]$ is maximized under $P_{\mu_i}(k) = P_{\mu_i}(k, l)$.
2. For $P_{\mu_i}(k, l)$, a corresponding $\eta_i(k, m)$ can be found for some m such that $J_t(\eta_i(k), P_{\mu_i}(k, l))$ is minimized under $\eta_i(k) = \eta_i(k, m)$.
3. If $\eta_i(k, j) = \eta_i(k, m)$, then the pair $\{\eta_i(k, m), P_{\mu_i}(k, l)\}$ is a Nash equilibrium.

Applying the above algorithm to example 1 yields:

1. For $\eta_i(k) = 1$, $P_{\mu_i}(k) = 1$ maximizes J_{μ_i} because

$$J_{\mu_i}(1, 1) = 10 \text{ is greater than } J_{\mu_i}(1, 0.8) = 8.$$

Then, for $P_{\mu_i}(k) = 1$, $\eta_i(k) = 1.2$ minimizes J_t because

$$J_t(1.2, 1) = 6 \text{ is less than } J_t(1, 1) = 9.$$

However, $\eta_i(k) = 1.2 \neq \eta_i(k) = 1$.

2. For $\eta_i(k) = 1.2$, $P_{\mu_i}(k) = 0.8$ maximizes J_{μ_i} because

$$J_{\mu_i}(1.2, 0.8) = 7 \text{ is greater than } J_{\mu_i}(1.2, 1) = 6.$$

Then, for $P_{\mu_i}(k) = 0.8$, $\eta_i(k) = 1.2$ minimizes because

$$J_t(1.2, 0.8) = 5 \text{ is less than } J_t(1, 0.8) = 10.$$

Since $\eta_i(k) = 1.2 = \eta_i(k) = 1.2$, $\{\eta_i(k), P_{\mu_i}(k)\} = \{1.2, 1\}$ is the Nash equilibrium.

A.6 Profiles used in the simulation

There are 8 DGs spread across the microgrid on Fig. 6. Usually, solar power of DGs differ from each other due to variable environmental conditions, such as a passing cloud or storm. Especially, if the microgrid is geographically expanded, the sunshine intense for different DGs will also be different. As such, PV profiles should account for such non consistencies. Figure 12 provides proposed PV profiles used in the numerical example. These profiles, reflect the environmental and geographical differences, which may exist among DGs.

The microgrid case of study of Fig. 6, has five feeders. To account for the different kinds of possible consumers, different loads have been assumed to be connected to each feeder as follows and shown in Fig. 13. Each plot in the figure means:

(1) Loads on feeder 1 represent industrial two shift workday.
(2) Loads on feeder 2 are assumed to be of a commercial area.
(3) Loads on feeder 3 represent an active night life area.
(4) Loads on feeders 4 and 5 are assumed to be of small residential areas.

Load profile of the main grid is also shown in Fig. 14.

The per unit cost of the conventional generators of the main grid is shown in Fig. 15. In this figure, P_G^* is the optimal operation point of the generators; that is the load on which they have the lowest cost. Due to the extra required fuel, the price increases quadratically beyond this point. Below this point also the cost per unit increases, however with a lower rate, due to the constant and permanent expenditures of generator stations such as human resources, maintenance fees and etc.

A.7 Details of finding game solution for the first hour

Here, the game approach for the first hour is provided to illustrate the game solution process. For the value of ΔE, microgrid chooses five values between higher and lower bounds to play the game. Higher and lower bounds are determined by the facts that storage cannot be charged beyond 1 P.U or be discharged below 0. Also, $|\Delta E| \leq$ 0.25 P.U, which is the charge and discharge rate limitation. As such, and regarding the initial storage of 0.5 P.U, the chosen values for the first hour are as follows:

$$\Delta E(1) = [-0.25 \quad -0.125 \quad 0 \quad 0.125 \quad 0.25].$$

For every ΔE, the microgrid power flow, P_μ, can be calculated using (12) and (23). As such and according to the PV/Load profiles:

$$P_\mu(1) = [0.0938 \quad -0.0312 \quad -0.1562 \quad -0.2812 \quad -0.4062]. \quad (55)$$

To calculate the cost function for the remaining hours, the P_μ^{avg} should be evaluated using (24) and PV profiles in Fig. 12:

$$P_\mu^{avg}(2 \to 24) = [0.0021 \quad 0.0076 \quad 0.013 \quad 0.0184 \quad 0.0239].$$

Then, according to the load profile of Fig. 14, the microgrid offers of $P_\mu(1)$ in (55) and using (38, 39), $P_G(1)$ and $P_G^{avg}(2 \to 24)$ are calculated as:

$$P_G(1) = [1.384 \quad 1.509 \quad 1.634 \quad 1.759 \quad 1.884],$$

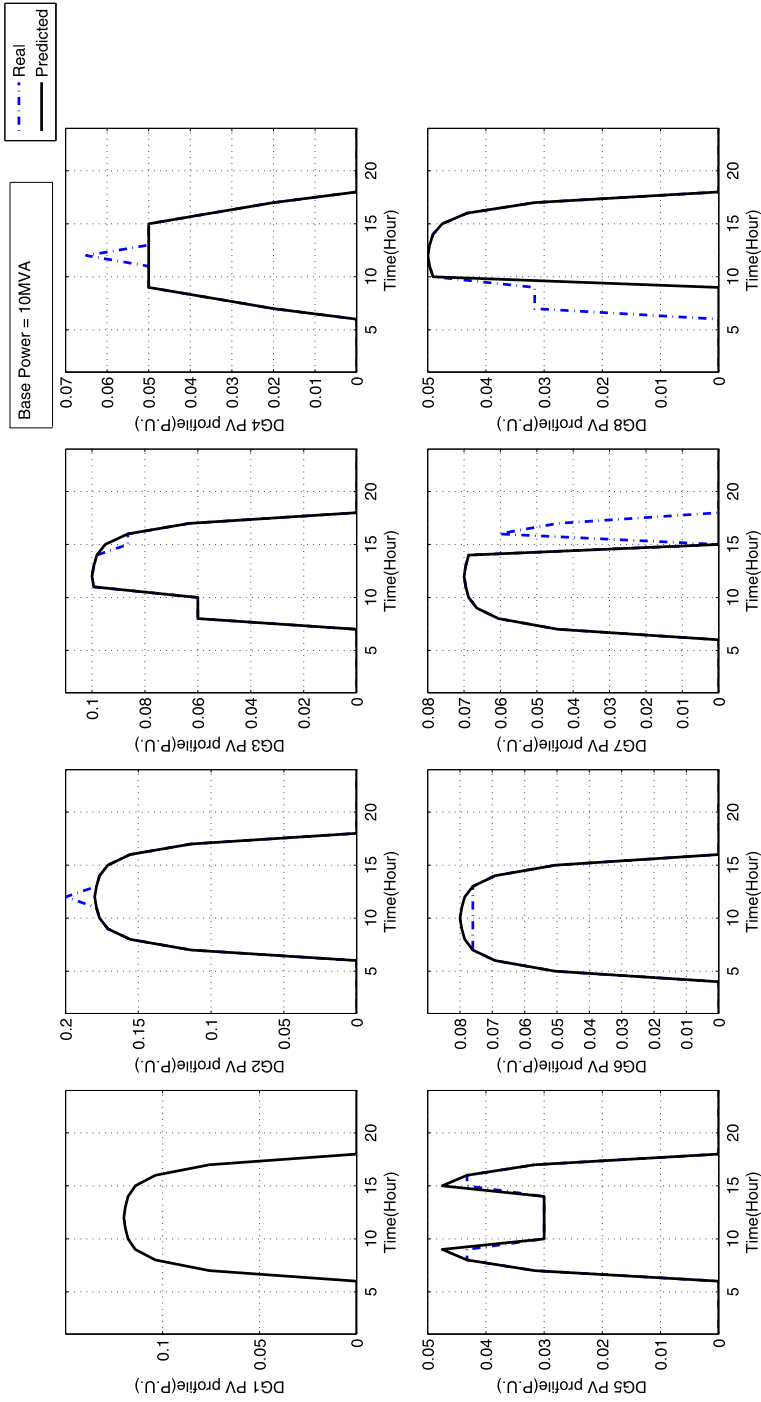**Fig. 12** PV profiles of DGs of the microgrid

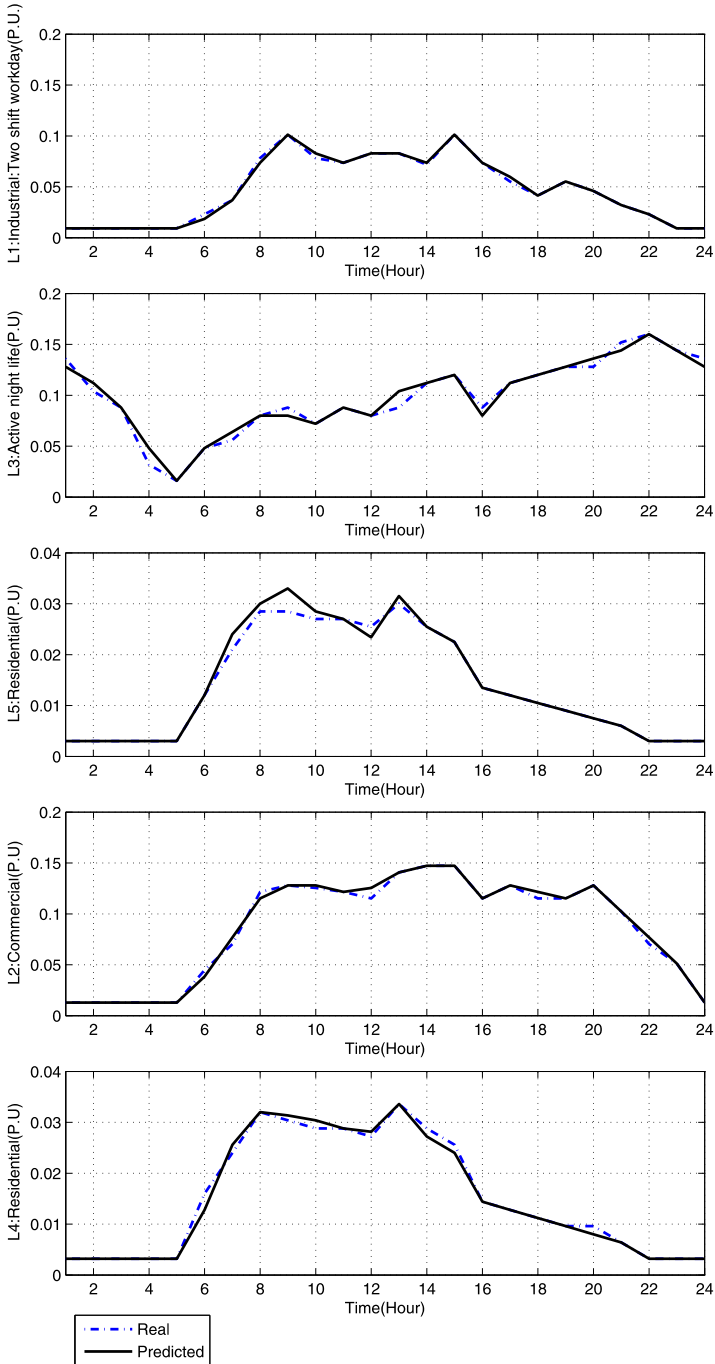**Fig. 13** Load profiles of different feeders
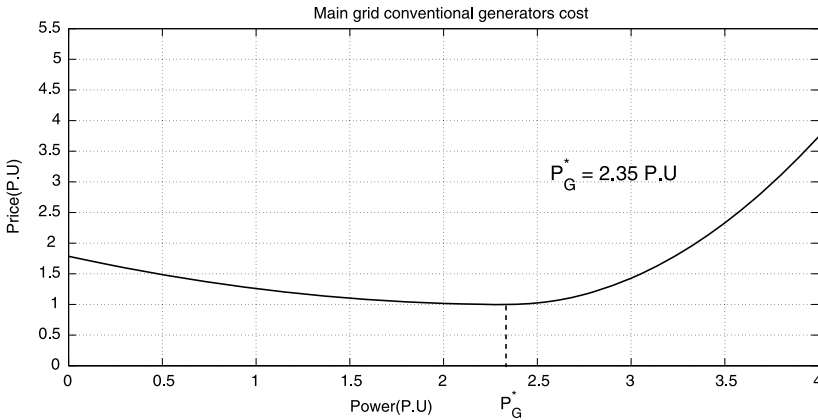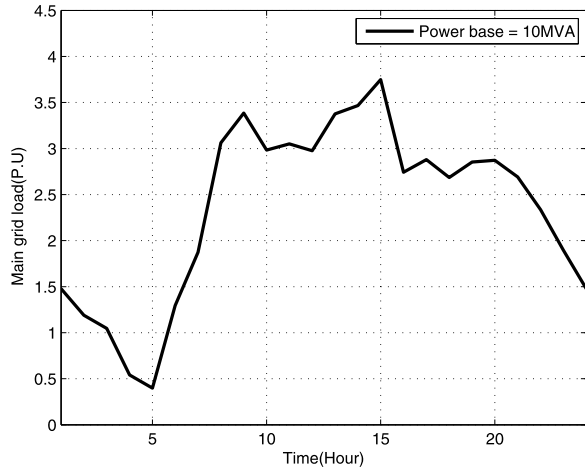
Fig. 14 Main grid load profile

Fig. 15 Conventional generation cost per unit

$$P_G^{avg}(2-24) = [2.3816 \quad 2.3762 \quad 2.3708 \quad 2.3653 \quad 2.3599].$$

The price, $\beta(1)$, that the main grid offers to the microgrid is calculated using (40). The default value of $\eta = 1$. To get the best possible price to offer, η is perturbed around the default value. The following five values of η are played against the microgrid proposed P_μ:

$$\eta(1) = [0.5 \quad 0.75 \quad 1 \quad 1.25 \quad 1.5].$$

To calculate $\beta^{avg}(2-23)$, $P_G^{avg}(2-23)$ is substituted into (40).

Moreover, $a(1)$ and $a^{avg}(2-23)$ are calculated from Fig. 15 for the $P_G(1)$ and $P_G^{avg}(2-24)$, respectively. As such, (18, 19) are written as follows for the first hour:

$$J_\mu(1) = \beta(1)P_\mu(1) + 23\beta^{avg}(2-23)P_\mu^{avg}(2-23),$$
$$J_t(1) = a(1)P_G(1) + \beta(1)P_\mu(1) + 23\{a^{avg}(2-23)P_G^{avg}(2-23)$$

Table 6 J_μ cost function game table

$J_\mu(1)$		$P_\mu(1)$				
		0.0858	−0.0392	−0.1642	−0.2892	−0.4142
$\eta(1)$	0.5	3.0126	3.2084	3.3487	3.4336	**3.4629**
	0.75	2.9479	3.2417	3.4522	3.5794	3.6234
	1	2.8833	3.2750	3.5556	3.7253	3.7839
	1.25	2.8187	3.3083	3.6591	3.8712	3.9445
	1.5	2.7541	3.3416	3.7626	4.0170	4.1050

Table 7 J_t cost function game table

$J_t(1)$		$P_\mu(1)$				
		0.0858	−0.0392	−0.1642	−0.2892	−0.4142
$\eta(1)$	0.5	59.1290	59.2822	59.3825	59.4315	**59.4309**
	0.75	59.0644	59.3155	59.4860	59.5774	59.5914
	1	58.9998	59.3488	59.5894	59.7233	59.7519
	1.25	58.9352	59.3821	59.6929	59.8691	59.9125
	1.5	58.8705	59.4154	59.7963	60.0150	60.0730

$$+ \beta^{avg}(2-23)P_\mu^{avg}(2-23)\}.$$

Therefore, the game matrix will be found as in Tables 6, 7 for the first hour. The Stackelberg solution for these matrices with the main grid as the leader yields $\eta = 0.5$ and $P_\mu = -0.4142$ as the solution. The same process is used for the remaining hours.

References

1. Alatrash, H., Mensah, A., Mark, E., Amarin, R., Enslin, J.: Generator emulation controls of photovoltaic inverters. In: Proceedings of the 8th International Conference on Power Electronics—ECCE Asia, pp. 2043–2050, Jeju, South Korea (2011)
2. Basar, T., Olsder, G.J.: Dynamic Noncooperative Game Theory, 2nd edn. SIAM, Philadelphia (1999)
3. Bilgin, H.F., Ermis, M.: Design and implementation of a current-source converter for use in industry applications of d-statcom. IEEE Trans. Power Electron. **25**, 1943–1957 (2010)
4. Bjorndal, M., Gribkovskaia, V., Jornsten, K.: Market power in a power market with transmission constraints. In: The Proceedings of the 7th International Conference on the European Energy Market, Madrid, Spain, pp. 1–6 (2010)
5. Carvalho, P.M.S., Correia, P.F., Ferreira, L.A.F.M.: Distributed reactive power generation control for voltage rise mitigation in distribution networks. IEEE Trans. Power Syst. **23**, 766–772 (2008)
6. Chinchuluun, A., Pardalos, P., Migdalas, A., Pitsoulis, L.: Pareto Optimality, Game Theory and Equilibria. Springer, Berlin (2008)
7. Ganguly, S., Sahoo, N.C., Das, D.: A novel multi-objective pso for electrical distribution system planning incorporating distributed generation. Energy Syst. **1**, 291–337 (2010)
8. Hasan, E., Galiana, F.: Fast computation of pure strategy Nash equilibria in electricity markets cleared by merit order. IEEE Trans. Power Syst. **25**, 722–728 (2010)
9. Holmes, M.: Introduction to Perturbation Methods. Springer, Berlin (1995)
10. Park, J.-B., Kim, B.M., Kim, J.-H., Jung, M.-H., Park, J.-K.: A continuous strategy game for power transactions analysis in competitive electricity markets. IEEE Trans. Power Syst. **16**, 847–855 (2001)

11. Kannan, A., Shanbhag, U.V., Kim, H.M.: Strategic behavior in power markets under uncertainty. Energy Syst. **2**, 115–141 (2010)
12. Katiraei, F., Iravani, M., Lehn, P.: Small-signal dynamics model of a micro-grid including conventional and electronically interfaced distributed resources. IET Gener. Transm. Distrib. **1**, 369–378 (2007)
13. Katiraei, F., Iravani, R., Hatziargyriou, N., Dimeas, A.: Microgrids management. IEEE Power Energy Mag. **6**, 54–65 (2008)
14. Khaitan, S.K., McCalley, J.D., Raju, M.: Numerical methods for on-line power system load flow analysis. Energy Syst. **1**, 273–289 (2010)
15. Khalil, H.K.: Nonlinear Systems, 3rd edn. Prentice-Hall, Upper Saddle River (2002)
16. Latorre, M., Granville, S.: The Stackelberg equilibrium applied to AC power systems—a non-interior point algorithm. IEEE Trans. Power Syst. **18**, 611–618 (2003)
17. Luh, P., Ho, Y., Muralidharan, R.: Load adaptive pricing: An emerging tool for electric utilities. IEEE Trans. Autom. Control **27**, 320–329 (1982)
18. Mohsenian-Rad, A., Wong, V., Jatskevich, J., Schober, R., Leon-Garcia, A.: Autonomous demand-side management based on game-theoretic energy consumption scheduling for the future smart grid. IEEE Trans. Smart Grid **1**, 320–331 (2010)
19. Molina, J., Zolezzi, J., Contreras, J., Rudnick, H., Reveco, J.: Nash-Cournot equilibria in hydrothermal electricity markets. IEEE Trans. Power Syst. **26**, 1089–1101 (2011)
20. Myerson, R.: Game Theory: Analysis of Conflict. Harvard University Press, Cambridge (1997)
21. Nash, J.: Equilibrium points in n-person games. Proc. Natl. Acad. Sci. USA **36**, 48–49 (1950)
22. Nash, J.: Non-cooperative games. Ann. Math. **54**, 286–295 (1951)
23. National Energy Technology Laboratory US Department of Energy Office of Electricity Delivery and Energy Reliability: A Vision for the Modern Grid (2007)
24. Pardalos, P., Grundel, D., Murphey, R.A., Prokopyev, O.: Cooperative Networks: Control and Optimization. Edward Elgar, Cheltenham Glos (2008)
25. Pozo, D., Contreras, J.: Finding multiple Nash equilibria in pool-based markets: A stochastic epec approach. IEEE Trans. Power Syst. **26**, 1744–1752 (2011)
26. Purchala, K., Meeus, L., Dommelen, D.V., Belmans, R.: Usefulness of DC power flow for active power flow analysis. In: The Proceedings of the IEEE 2005 Power Engineering Society General Meeting, pp. 454–459, San Francisco, CA, USA (2005)
27. Qu, Z.: Cooperative Control of Dynamical Systems. Springer, London (2009)
28. Ren, W., Beard, R.W.: Distributed Consensus in Multi-vehicle Cooperative Control: Theory and Applications. Springer, London (2009)
29. Schauder, C., Mehta, H.: Vector analysis and control of the advanced static VAR compensators. IEE Proc., Gener. Transm. Distrib. **140**, 299–306 (1993)
30. Simaan, M., Cruz, J.: Additional aspects of the Stackelberg strategy in nonzero-sum games. J. Optim. Theory Appl. **11**, 613–626 (1973)
31. Simaan, M., Cruz, J.: On the Stackelberg strategy in nonzero-sum games. J. Optim. Theory Appl. **11**, 533–555 (1973)
32. Stackelberg, H.F.V.: The Theory of the Market Economy. William Hodge, London (1952)
33. Vale, Z., Morais, H., Khodr, H.: Intelligent multi-player smart grid management considering distributed energy resources and demand response. In: Proceedings of the IEEE Power and Energy Society General Meeting, pp. 1–7, Porto, Portugal (2010)
34. Xin, H., Qu, Z., Seuss, J., Maknouninejad, A.: A self-organizing strategy for power flow control of photovoltaic generators in a distribution network. IEEE Trans. Power Syst. **26**, 1462–1473 (2011)
35. Zhao, J., Brereton, B., Montalvo, M.: Gaming-based reserve constraint penalty factor analysis. IEEE Trans. Power Syst. **26**, 616–626 (2011)
36. Zmood, D.N., Holmes, D.G.: Improved voltage regulation for current-source inverters. IEEE Trans. Ind. Appl. **37**, 1028–1036 (2001)